



# Stochastic analysis of saturated–unsaturated flow in heterogeneous media by combining Karhunen-Loeve expansion and perturbation method

Jinzhong Yang<sup>a</sup>, Dongxiao Zhang<sup>b,c,\*</sup>, Zhiming Lu<sup>b</sup>

<sup>a</sup>National Key Laboratory of Water Resources and Hydropower Engineering Sciences, Wuhan University, Wuhan, China

<sup>b</sup>Hydrology, Geochemistry, and Geology Group (EES-6), Los Alamos National Laboratory, Los Alamos, NM 87545, USA

<sup>c</sup>Mewbourne School of Petroleum & Geological Eng, The University of Oklahoma, Norman, OK73019, USA

Received 8 April 2003; revised 30 September 2003; accepted 20 October 2003

## Abstract

In this study, a stochastic model for transient saturated–unsaturated flow is developed based on the Karhunen-Loeve expansion of the input random soil properties combined with a perturbation method. The log-transformed saturated hydraulic conductivity  $f(\mathbf{x})$  and the soil pore size distribution parameter  $\alpha(\mathbf{x})$  are assumed to be normal random functions with known covariances. We decompose  $f(\mathbf{x})$  and  $\alpha(\mathbf{x})$  as infinite series in a set of orthogonal normal random variables by the Karhunen-Loeve expansion and expand the pressure head as polynomial chaos with the same set of orthogonal random variables. The perfectly correlated and uncorrelated cases between  $f(\mathbf{x})$  and  $\alpha(\mathbf{x})$  are studied. By using the Karhunen-Loeve expansion of the input random parameters, polynomial chaos decomposition of pressure head, and the perturbation method, the saturated–unsaturated flow equation and the corresponding initial and boundary conditions are represented by a series of partial differential equations in which the dependent variables are the deterministic coefficients of the polynomial chaos expansion. Once the partial differential equations are solved subsequently by a numerical method, the random representation of pressure head is obtained by combining the deterministic coefficients obtained and the random variables from the Karhunen-Loeve expansion of the input random functions. The moments of pressure head and water content are determined directly from the random representation of the pressure head. We demonstrated the applicability of the proposed KL-based stochastic model with some examples of unsaturated and saturated–unsaturated flow in two dimensions, and compared the results with those from the moment-based stochastic model. It is shown that the KL-based models are more computationally efficient than the conventional moment-based models.

© 2004 Elsevier B.V. All rights reserved.

**Keywords:** Stochastic modeling; Saturated–unsaturated flow; Karhunen-Loeve expansion; Perturbation method; Numerical analysis; Vadose zone

## 1. Introduction

It has been recognized that medium heterogeneity significantly impacts fluid flow and solute transport in the subsurface. The vadose zone connects

\* Corresponding author. Tel.: +1-405-325-5928; fax: +1-405-325-7477.

E-mail addresses: [cshy@public.wh.hb.cn](mailto:cshy@public.wh.hb.cn) (J. Yang); [donzhang@ou.edu](mailto:donzhang@ou.edu) (D. Zhang); [zhiming@lanl.gov](mailto:zhiming@lanl.gov) (Z. Lu).

the hydrologic processes above ground and the groundwater. Movement of water and pollutants in the vadose zone affects the growth of vegetation, the amount of recharge and evapotranspiration, and the overall quality of water. Spatial variability of hydraulic properties in the vadose zone is one of the important factors that control the migration rate and path of water and pollutants. Because of incomplete knowledge about the spatial distribution of hydraulic properties, prediction of water flow and transport processes in the vadose zone always involves some degree of uncertainty. To address the uncertainty, stochastic modeling of flow and solute transport processes becomes necessary (Bresler and Dagan, 1981; Dagan and Bresler, 1979; Yeh et al., 1985c; Yang et al., 1997). Field observations show that the hydraulic properties of soils vary significantly with spatial locations even for the same soil type. Despite this spatial variability, medium properties, including fundamental parameters such as permeability and porosity, are usually observed only at a few locations due to the high cost associated with subsurface measurements. This combination of significant spatial heterogeneity with a relatively small number of observations leads to uncertainty about the values of medium properties and thus to uncertainty in predicting flow and solute transport in such media. It has been recognized that the theory of stochastic processes provides a useful method for evaluating flow and transport uncertainties.

In the last 2 decades, many stochastic theories have been developed to study the effects of spatial variability on flow and transport in both saturated (Gelhar and Axness, 1983; Winter et al., 1984; Dagan, 1984, 1989; Neuman et al., 1987; Zhang, 2002) and unsaturated zones (Jury, 1982; Yeh et al., 1985a,b; Mantoglou and Gelhar, 1987; Mantoglou, 1992; Russo, 1993, 1995; Yang et al., 1996a,b, 1997; Zhang and Winter, 1998; Zhang, 1998, 1999, 2002; Zhang and Lu, 2002; Lu and Zhang, 2002). In the unsaturated zone the problem is further complicated by the fact that the flow equations are nonlinear because unsaturated hydraulic conductivity depends on pressure head. Many earlier stochastic studies focused on steady state, gravity-dominated unsaturated flow in unbounded domains. Under these conditions the unsaturated flow field is stationary, and hence analytical or semi-analytical solutions are

possible. Zhang and Winter (1998) developed a general nonstationary stochastic approach for steady state unsaturated flow in bounded domains. On the basis of some one- and two-dimensional examples they found that the simpler, gravity-dominated flow models may provide good approximations for flow in vadose zones of large thickness and/or coarse-textured soils. Zhang et al. (1998) studied the impact of different constitutive models on steady state unsaturated flow in both bounded and unbounded domains. Liedl (1994) proposed a perturbation model for transient unsaturated flow. The results of the model are a set of partial differential equations governing the statistical moments of saturation. Liedl implemented the model in one dimension. Li and Yeh (1998) studied transient unsaturated flow in heterogeneous porous media using a vector state-space approach and investigated the behavior of head variances for transient unsaturated flow in two dimensions. Zhang (1999) studied transient unsaturated flow for nonstationary situation and derived partial differential equations governing the statistical moments by perturbation expansions and then implemented these equations by the method of finite differences. Zhang and Lu (2002) extended the work of Zhang (1999) to coupled unsaturated flow and saturated flow, and to include randomness in the boundary/initial conditions and source/sink terms that can be nonstationary in space and time. Lu and Zhang (2002) studied the unsaturated flow on the base of the van Genuchten–Mualem constitutive relation and investigated the impacts of different constitutive models on statistic moments.

The analytical and semi-analytical results of the unsaturated water flow in random distributed soils (Yeh et al., 1985a,b; Mantoglou and Gelhar, 1987; Russo, 1993) lead to the general understanding of the stochastic flow characteristics. However, because of the complexity of the soil distribution and the boundary conditions in the real world, the results can only be used for the analysis of simplified problems. The state-space approach (Li and Yeh, 1998) and the perturbation moment equation approach (Mantoglou, 1992; Zhang, 1999; Zhang and Lu, 2002) can be used for more general situations with complex soil properties, different shapes of the simulation domain, realistic boundary/initial conditions, and the presence of internal sink/source. The challenge is

the computational effort even only when the first order moment is evaluated.

Recent research developments in stochastic finite elements have also headed in the direction of numerical analysis of stochastic mechanics with spatially distributed random material properties and random loads. In this approach, the governing stochastic partial differential equation is discretized in the Euclidian physical dimensions by a finite element procedure and the randomness is involved in the stochastic global stiffness matrix and vector of the resultant ordinary differential equation system (Deodatis, 1989; Ghanem and Spanos, 1991a,b; Ghanem and Kruger, 1996; Matthies et al., 1997; Ghanem, 1998, 1999a–c; Ghanem and Dham, 1998). The resulting matrix equation can be solved along the line of Monte Carlo simulation, perturbation method and spectral expansion method. In the spectral stochastic finite element method, the spatial random media property in elements is expressed by the Karhunen-Loeve expansion and the randomness of the system is viewed as an additional dimension in which a set of basic functions is defined, which is referred to as polynomial chaos (Wiener, 1938). The same procedure as the deterministic Galerkin finite element method is applied for the resulting residual to be orthogonal to the approximating space spanned by the base of the polynomial chaos. The resulting deterministic system of algebraic equation can be used for the solution of the deterministic coefficients of the polynomial chaos expansion. The coefficient matrix is of order  $n \times P$ , where  $n$  is the number of nodes and  $P$  is the number of polynomials in the truncated polynomial chaos expansion (Ghanem and Spanos, 1991b). This method can be efficient because only a small number of terms in the polynomial chaos expansion are needed for most engineering problems.

In this work, the stochastic saturated–unsaturated flow equation with the spatial random hydraulic conductivity and pore size distribution parameter is solved based on the combination of Karhunen-Loeve expansion of the random inputs of the media properties and a perturbation method. Roy and Grilli (1997) solved the steady state saturated flow equation by using the Karhunen-Loeve expansion combined with the perturbation method and obtained the mean head and the head variance in first and second order in  $\sigma_f$ , respectively, where  $\sigma_f$  is the standard deviation of

the log-transformed saturated hydraulic conductivity. Zhang and Lu (2004) solved the transient saturated flow equation and obtained the mean head to fourth order in  $\sigma_f$  and the head covariance to third order in  $\sigma_f^2$ . The present work is different from those of Roy and Grilli (1997); Zhang and Lu (2004) in that the steady and transient saturated–unsaturated flow problem are solved with more than one spatial random parameters, which are treated as perfectly correlated or uncorrelated random functions. The focus of our consideration is the efficiency of the method compared with the commonly used moment-based method for the nonlinear stochastic flow problems.

## 2. Basic equations of the saturated–unsaturated flow problem

We consider transient flow in saturated–unsaturated media satisfying the following continuity equation

$$C(\mathbf{x}, t) \frac{\partial h(\mathbf{x}, t)}{\partial t} = \nabla[K(\mathbf{x}, t)\nabla(h(\mathbf{x}, t) + z)] + g(\mathbf{x}, t) \quad (1)$$

subject to initial and boundary conditions

$$\begin{aligned} -\{K(\mathbf{x})\nabla[h(\mathbf{x}, t) + z] \cdot \mathbf{n}\}|_{\Gamma_2} &= Q_n(\mathbf{x}, t) \\ h(\mathbf{x}, t)|_{\Gamma_1} &= h_{\Gamma_1}(\mathbf{x}, t) \quad h(\mathbf{x}, t)|_{t=0} = h_{\text{ini}}(\mathbf{x}) \end{aligned} \quad (2)$$

where  $h(\mathbf{x}, t) + z$  is the total hydraulic head,  $h(\mathbf{x}, t)$  is the pressure head,  $g(\mathbf{x}, t)$  is the fluid source or sink term,  $C(\mathbf{x}, t)$  is the specific moisture capacity, and  $K(\mathbf{x}, t)$  is the unsaturated hydraulic conductivity.  $Q_n(\mathbf{x}, t)$ ,  $h_{\Gamma_1}(\mathbf{x}, t)$  and  $h_{\text{ini}}(\mathbf{x})$  are the flux out of the Neumann boundary  $\Gamma_2$ , the pressure head at the first type boundary  $\Gamma_1$ , and the initial pressure head distribution in the domain, respectively. For simplicity,  $g(\mathbf{x}, t)$ ,  $Q_n(\mathbf{x}, t)$ ,  $h_{\Gamma_1}(\mathbf{x}, t)$  and  $h_{\text{ini}}(\mathbf{x})$  are treated as deterministic functions.

$K(\mathbf{x}, t)$  and  $C(\mathbf{x}, t)$  are functions of  $h(\mathbf{x}, t)$  and Eq. (1) is nonlinear. Some models are needed to describe the constitutive relationships of  $K(\mathbf{x}, t)$  and  $C(\mathbf{x}, t) = d\theta/dh$ , where  $\theta$  is the water content. No universal models are available for the constitutive relationships. Instead, several empirical models are usually used, including the Gardner–Russo model (Gardner, 1958; Russo, 1988), the Brooks–Corey model (Brooks and Corey, 1964), and the van Genuchten–Mualem model (van Genuchten, 1980).

In most existing stochastic models of unsaturated flow, the Gardner–Russo model is used because of its simplicity. Although the Brooks–Corey model may have certain mathematical advantages over the Gardner–Russo model in low-order stochastic analyses (Zhang et al., 1998), we use the latter to facilitate comparisons with literature results. The Gardner–Russo model reads as

$$K(\mathbf{x}, t) = \begin{cases} K_s(\mathbf{x})\exp[\alpha(\mathbf{x})h(\mathbf{x}, t)] & h < 0 \\ K_s(\mathbf{x}) & h \geq 0 \end{cases} \quad (3)$$

$$\theta_e(\mathbf{x}, t) = \begin{cases} (\theta_s - \theta_r)\left\{\exp\left[\frac{1}{2}\alpha(\mathbf{x})h(\mathbf{x}, t)\right] \times \left[1 - \frac{1}{2}\alpha(\mathbf{x})h(\mathbf{x}, t)\right]\right\}^{2/(m+2)} & h < 0 \\ \theta_s - \theta_r, & h \geq 0 \end{cases}$$

where  $\theta_e$ ,  $\theta_r$ , and  $\theta_s$  are the effective, residual, and saturated water content, respectively,  $K_s(\mathbf{x})$  is the saturated hydraulic conductivity,  $\alpha(\mathbf{x})$  is the soil parameter related to the pore size distribution, and  $m$  is a parameter related to tortuosity. For simplicity, we let  $m = 0$  in this study. In this case, the specific soil water capacity  $C(\mathbf{x}, t)$  can be expressed as

$$C(\mathbf{x}, t) = \begin{cases} -\frac{\theta_s - \theta_r}{4}\alpha^2(\mathbf{x})h(\mathbf{x}, t) \times \exp\left[\frac{1}{2}\alpha(\mathbf{x})h(\mathbf{x}, t)\right] & h \leq 0, \\ S_s & h > 0 \end{cases} \quad (4)$$

where  $S_s$  is the specific storage.

The extension to the case of  $m \neq 0$  can be made by following the treatment of Zhang et al. (1998) for steady state unsaturated flow. The variabilities of  $\theta_s$  and  $\theta_r$  are likely to be small compared to that of the effective water content  $\theta_e$ . In this study,  $\theta_s$  and  $\theta_r$  are assumed to be deterministic constants. The soil pore size distribution parameter  $\alpha(\mathbf{x})$  and the log-transformed saturated hydraulic conductivity  $f(\mathbf{x}) = \ln \times K_s(\mathbf{x})$  are treated as random space functions. They are assumed to be normal random functions with known covariances.

When the soil properties  $f(\mathbf{x})$  and  $\alpha(\mathbf{x})$  are treated as random space functions, the governing Eqs. (1)–(2) become a set of stochastic partial differential

equations whose solutions are no longer deterministic values but random functions with probability distributions related to the random inputs. In Section 3, we decompose the input random soil properties  $f(\mathbf{x})$  and  $\alpha(\mathbf{x})$  by Karhunen-Loeve expansion and determine the random representation of the pressure head, which is related to the random variables in the Karhunen-Loeve expansion. On the basis of the random representation of the pressure head, the statistical moments can be evaluated by simple manipulations.

### 3. Mathematical characterization of random space functions

#### 3.1. Karhunen-Loeve expansion of random soil parameters

The Karhunen-Loeve expansion of a random space function  $\phi(\mathbf{x}, \omega)$  is based on the spectral expansion of its covariance function  $C_{\phi\phi}(\mathbf{x}, \mathbf{y})$ , where,  $\mathbf{x}$  and  $\mathbf{y}$  denote spatial coordinates at different spatial points,  $\omega$  varies in probability space. The covariance function, being symmetrical and positive definite, has mutually orthogonal eigenfunctions that form a complete set spanning the function space to which  $\phi(\mathbf{x}, \omega)$  belongs. It can be shown that if this deterministic set of functions is used to represent the random function  $\phi(\mathbf{x}, \omega)$ , the random coefficients used in the expansion are also orthogonal (Ghanem and Spanos, 1991b). The expansion then takes the following form:

$$\begin{aligned} \phi(\mathbf{x}, \omega) &= \bar{\phi}(\mathbf{x}) + \sum_{i=1}^{\infty} \sqrt{\lambda_i} \phi_i^*(\mathbf{x}) \xi_i(\omega) \\ &= \bar{\phi}(\mathbf{x}) + \sum_{i=1}^{\infty} \phi_i(\mathbf{x}) \xi_i(\omega), \end{aligned} \quad (5)$$

where  $\bar{\phi}(\mathbf{x})$  denotes the mean of the random space function  $\phi(\mathbf{x}, \omega)$ , and  $\{\xi_i(\omega)\}$  form a set of orthogonal random variables. Furthermore,  $\{\phi_i^*(\mathbf{x})\}$  are the eigenfunctions and  $\{\lambda_i\}$  are the corresponding eigenvalues of the covariance kernel, which can be solved from the following integral equation:

$$\int_{\Omega} C_{\phi\phi}(\mathbf{x}, \mathbf{y}) \phi^*(\mathbf{y}) d\mathbf{y} = \lambda \phi^*(\mathbf{x}) \quad (6)$$

where  $\Omega$  denotes the spatial domain. The most important aspect of this spectral representation is that the spatial random fluctuations have been decomposed into a set of deterministic functions multiplying random variables. If the random function  $\phi(\mathbf{x}, \omega)$  is Gaussian, then the random variables  $\{\xi_i(\omega)\}$  form an orthogonal Gaussian vector. The Karhunen-Loeve expansion is mean square convergent irrespective of the probabilistic structure of the process being expanded, provided that it has a finite variance (Loeve, 1977; Ghanem and Spanos, 1991b).

Since there is no justifiable data for the statistical relationship between  $f(\mathbf{x})$  and  $\alpha(\mathbf{x})$ , we carry out the analysis by assuming either perfect or zero correlation between  $f(\mathbf{x})$  and  $\alpha(\mathbf{x})$ . For the perfectly correlated case,  $\alpha(\mathbf{x})$  can be expressed in terms of  $f(\mathbf{x})$ . Therefore,  $f(\mathbf{x})$  and  $\alpha(\mathbf{x})$  can be decomposed by Karhunen-Loeve expansion on the same set of a normal random basis  $\{\zeta_i(\omega)\}$ . If  $f(\mathbf{x})$  and  $\alpha(\mathbf{x})$  are uncorrelated, they can be decomposed by the Karhunen-Loeve expansion based on two sets of uncorrelated random bases  $\{\xi_i(\omega)\}$  and  $\{\eta_i(\omega)\}$ , respectively. We arrange  $\{\xi_i(\omega)\}$  and  $\{\eta_i(\omega)\}$  as  $\{\zeta_i(\omega)\} = \{\xi_i(\omega), \eta_i(\omega)\}$  and  $\{\zeta_i(\omega)\}$  will be used as a basis for the expansion of pressure head.

For the separable exponential covariance function of a random space function  $\phi(\mathbf{x}, \omega)$  in two-dimensional case,

$$C_{\phi\phi}(\mathbf{x}, \mathbf{y}) = \sigma_\phi^2 \exp\left(-\frac{|x_1 - y_1|}{\gamma_1} - \frac{|x_2 - y_2|}{\gamma_2}\right), \quad (7)$$

where  $\mathbf{x} = (x_1, x_2)$ ,  $\mathbf{y} = (y_1, y_2)$ , the eigenvalues and eigenfunctions can be found analytically for the rectangular domain  $\Omega = \{(x_1, x_2) : 0 \leq x_1 \leq L_1, 0 \leq x_2 \leq L_2\}$  and expressed as (Zhang and Lu, 2004)

$$\lambda_i = \frac{4\gamma_1\gamma_2\sigma_\phi^2}{(\gamma_1^2\omega_{1,m}^2 + 1)(\gamma_2^2\omega_{2,n}^2 + 1)}, \quad (8)$$

$$\phi_i^* = \phi_{1,m}(x_1)\phi_{2,n}(x_2), \quad (9)$$

where  $\sigma_\phi^2$  is the variance of the random space function  $\phi(\mathbf{x}, \omega)$ ,  $\gamma_k$  is correlation length of  $\phi(\mathbf{x}, \omega)$  in the direction  $x_k$ ,  $k = 1, 2$ , and

$$\phi_{k,i}(x_k) = \frac{\gamma_k \omega_{k,i} \cos(\omega_{k,i} x_k) + \sin(\omega_{k,i} x_k)}{\sqrt{(\gamma_k^2 \omega_{k,i}^2 + 1)L_k/2 + \gamma_k}}, \quad (10)$$

$k = 1, 2, i = 1, 2, 3, \dots$

$\omega_{k,i}$  are the positive roots of the following characteristic equations

$$(\gamma_k \omega_k - 1) \sin(\omega_k L_k) = 2\gamma_k \omega_k \cos(\omega_k L_k), \quad (11)$$

$k = 1, 2$

We first solve (11) to get the solutions  $\{\omega_{1,i}\}$  and  $\{\omega_{2,i}\}$ . Here we assume that the indices  $m$  and  $n$  in Eqs. (8) and (9) are mapped to  $i$  such a way that eigenvalues  $\lambda_i$  form a series whose terms are nonincreasing.

### 3.2. Polynomial chaos expansion of pressure head

The covariance function of the solution process is not known a priori, and hence the Karhunen-Loeve expansion cannot be used to represent it. Since the solution process is a function of the soil properties  $f(\mathbf{x})$  and  $\alpha(\mathbf{x})$ , the pressure head  $h(\mathbf{x}, t)$  can be formally expressed as some nonlinear functional of the set  $\{\zeta_i(\omega)\}$  used to represent the soil randomness. It has been shown that this functional dependence can be expanded in terms of polynomials in Gaussian random variables, referred to as polynomial chaos (Cameron and Martin, 1947)

$$h(\mathbf{x}, t) = H^{(0)}(\mathbf{x}, t) + \sum_{i=1}^{\infty} H_i(\mathbf{x}, t) \Gamma_1(\zeta_i) + \sum_{i=1}^{\infty} \sum_{j=1}^i H_{ij}(\mathbf{x}, t) \Gamma_2(\zeta_i, \zeta_j) + \sum_{i=1}^{\infty} \sum_{j=1}^i \sum_{k=1}^j H_{ijk}(\mathbf{x}, t) \Gamma_3(\zeta_i, \zeta_j, \zeta_k) + \dots, \quad (12)$$

where  $\Gamma_n(\zeta_{i_1}, \zeta_{i_2}, \zeta_{i_3}, \dots, \zeta_{i_n})$  is the  $n$ th order polynomial chaos, which in general can be expressed as the Hermite polynomial:

$$\begin{aligned} \Gamma_n(\zeta_{i_1}, \zeta_{i_2}, \zeta_{i_3}, \dots, \zeta_{i_n}) &= \exp\left(\frac{1}{2} \sum_{i=1}^n \zeta_i \zeta_i\right) (-1)^n \frac{\partial^n}{\partial \zeta_{i_1} \partial \zeta_{i_2} \dots \partial \zeta_{i_n}} \\ &\times \exp\left(-\frac{1}{2} \sum_{i=1}^n \zeta_i \zeta_i\right). \end{aligned}$$

All elements in  $\{\Gamma_n(\zeta_{i_1}, \zeta_{i_2}, \zeta_{i_3}, \dots, \zeta_{i_n})\}$  are mutually orthogonal and form a basis in second

order random function space. Any element of the set  $\{I_n(\zeta_{i_1}, \zeta_{i_2}, \zeta_{i_3}, \dots, \zeta_{i_n})\}$  is a polynomial of  $(\zeta_{i_1}, \zeta_{i_2}, \zeta_{i_3}, \dots, \zeta_{i_n})$ . Therefore, we can rearrange the expansion of  $h(\mathbf{x}, t)$  as the summation of all possible polynomials of  $(\zeta_{i_1}, \zeta_{i_2}, \zeta_{i_3}, \dots, \zeta_{i_n})$  (Zhang and Lu, 2004)

$$\begin{aligned}
 h(\mathbf{x}, t) &= h^{(0)}(\mathbf{x}, t) + \sum_{i=1}^{\infty} h_i(\mathbf{x}, t)\zeta_i + \sum_{i,j=1}^{\infty} h_{ij}(\mathbf{x}, t)\zeta_i\zeta_j \\
 &+ \sum_{i,j,k=1}^{\infty} h_{ijk}(\mathbf{x}, t)\zeta_i\zeta_j\zeta_k + \dots \\
 &+ \sum_{i_1, i_2, \dots, i_m=1}^{\infty} \left\{ h_{i_1, i_2, \dots, i_m}(\mathbf{x}, t) \left[ \prod_{j=1}^m \zeta_{i_j} \right] \right\} + \dots \\
 &= h^{(0)}(\mathbf{x}, t) + h^{(1)}(\mathbf{x}, t) + h^{(2)}(\mathbf{x}, t) + \dots \quad (13)
 \end{aligned}$$

The infinite series of Eqs. (12) and (13) are equivalent after rearranging terms. The first summation in Eq. (13) is the linear and Gaussian part of the random function  $h(\mathbf{x}, t)$ . A complete probability characterization of the random function  $h(\mathbf{x}, t)$  is obtained if all the deterministic coefficients  $(h^{(0)}(\mathbf{x}, t), h_i(\mathbf{x}, t), h_{ij}(\mathbf{x}, t), h_{ijk}(\mathbf{x}, t), \dots, i, j, k, \dots = 1, 2, \dots)$  in (13) have been calculated.

#### 4. Expansion of the random soil parameters

The log-transformed unsaturated soil conductivity  $Y(\mathbf{x}, t) = \ln K(\mathbf{x}, t)$  can be written as:

$$Y(\mathbf{x}, t) = \ln[K(\mathbf{x}, t)] = f(\mathbf{x}) + \alpha(\mathbf{x})h(\mathbf{x}, t) \quad h \leq 0. \quad (14)$$

The  $f(\mathbf{x})$  and  $\alpha(\mathbf{x})$  are inputs of the system with known covariance  $C_{ff}(\mathbf{x}, \mathbf{y})$  and  $C_{\alpha\alpha}(\mathbf{x}, \mathbf{y})$ , respectively. We can write

$$\begin{aligned}
 f(\mathbf{x}) &= \bar{f}(\mathbf{x}) + f'(\mathbf{x}) \\
 \alpha(\mathbf{x}) &= \bar{\alpha}(\mathbf{x}) + \alpha'(\mathbf{x}),
 \end{aligned} \quad (15)$$

where  $\bar{f}(\mathbf{x})$  and  $\bar{\alpha}(\mathbf{x})$  are the means of  $f(\mathbf{x})$  and  $\alpha(\mathbf{x})$ ,  $f'(\mathbf{x})$  and  $\alpha'(\mathbf{x})$  the zero mean Gaussian random functions, which can be expressed by the Karhunen-Loeve expansion.

By substituting (13) and (15) into (14), we have

$$Y(\mathbf{x}, t) = Y^{(0)}(\mathbf{x}, t) + Y^{(1)}(\mathbf{x}, t) + Y^{(2)}(\mathbf{x}, t) + \dots \quad (16)$$

where

$$Y^{(0)}(\mathbf{x}, t) = \bar{f}(\mathbf{x}) + \bar{\alpha}(\mathbf{x})h^{(0)}(\mathbf{x}, t) \quad (17)$$

$$Y^{(1)}(\mathbf{x}, t) = f'(\mathbf{x}) + \bar{\alpha}(\mathbf{x})h^{(1)}(\mathbf{x}, t) + h^{(0)}(\mathbf{x}, t)\alpha'(\mathbf{x})$$

$$Y^{(2)}(\mathbf{x}, t) = \bar{\alpha}(\mathbf{x})h^{(2)}(\mathbf{x}, t) + \alpha'(\mathbf{x})h^{(1)}(\mathbf{x}, t)$$

By substituting (13) and (15) into (4), we obtain

$$\begin{aligned}
 C(\mathbf{x}, t) &= -\frac{\theta_s - \theta_r}{4} \alpha^2(\mathbf{x})h(\mathbf{x}, t)\exp\left[\frac{1}{2}\alpha(\mathbf{x})h(\mathbf{x}, t)\right] \\
 &= C^{(0)}(\mathbf{x}, t) + C^{(1)}(\mathbf{x}, t) + C^{(2)}(\mathbf{x}, t) + \dots \quad (18)
 \end{aligned}$$

The arguments  $(\mathbf{x}, t)$  are omitted in the following expressions. The first three terms in (18) can be expressed as

$$\begin{aligned}
 C^{(0)} &= \bar{C}\bar{\alpha}^2h^{(0)}, \quad C^{(1)} = C_{11}h^{(1)} + C_{12}\alpha', \\
 C^{(2)} &= C_{21}h^{(2)} + C_{22}(h^{(1)})^2 + C_{23}\alpha'h^{(1)} + C_{24}\alpha'^2,
 \end{aligned} \quad (19)$$

where

$$C_{11} = \bar{C} \left[ \bar{\alpha}^2 + \frac{1}{2}\bar{\alpha}^3h^{(0)} \right],$$

$$C_{12} = \bar{C} \left[ 2\bar{\alpha}h^{(0)} + \frac{1}{2}\bar{\alpha}^2(h^{(0)})^2 \right]$$

$$C_{21} = \bar{C} \left[ \bar{\alpha}^2 + \frac{1}{2}\bar{\alpha}^3h^{(0)} \right],$$

$$C_{22} = \bar{C} \left[ \frac{1}{2}\bar{\alpha}^3 + \frac{1}{8}\bar{\alpha}^4h^{(0)} \right]$$

$$C_{23} = \bar{C} \left[ 2\bar{\alpha} + 3\bar{\alpha}^2h^{(0)} + \frac{3}{2}\bar{\alpha}^3(h^{(0)})^2 \right],$$

$$C_{24} = \bar{C} \left[ h^{(0)} + \frac{3}{2}\bar{\alpha}(h^{(0)})^2 + \frac{3}{4}\bar{\alpha}^2(h^{(0)})^3 \right]$$

$$\bar{C} = -\frac{\theta_s - \theta_r}{4} \exp\left[\frac{1}{2}\bar{\alpha}h^{(0)}\right].$$

The terms  $\exp(-Y)$  and  $\exp(Y)$  can be expressed as

$$\begin{aligned}
 e^{-Y} &= e^{-Y^{(0)}}(q^{(0)} + q^{(1)} + q^{(2)} + \dots) \\
 e^Y &= e^{Y^{(0)}}(p^{(0)} + p^{(1)} + p^{(2)} + \dots),
 \end{aligned} \quad (20)$$

where

$$\begin{aligned} q^{(0)} &= 1, \quad q^{(1)} = -Y^{(1)}, \quad q^{(2)} = -Y^{(2)} + \frac{1}{2}Y^{(1)}Y^{(1)} \\ p^{(0)} &= 1, \quad p^{(1)} = Y^{(1)}, \quad p^{(2)} = Y^{(2)} + \frac{1}{2}Y^{(1)}Y^{(1)} \end{aligned} \quad (21)$$

#### 4.1. Perfectly correlated $f(\mathbf{x})$ and $\alpha(\mathbf{x})$

When perfectly correlated, normally distributed random functions  $f(\mathbf{x})$  and  $\alpha(\mathbf{x})$  can be expanded as

$$\begin{aligned} f^l(\mathbf{x}) &= \sum_{i=1}^{\infty} f_i(\mathbf{x})\xi_i(\omega), \\ \alpha^l(\mathbf{x}) &= \sum_{i=1}^{\infty} \alpha_i(\mathbf{x})\xi_i(\omega), \end{aligned} \quad (22)$$

where  $\{\xi_i\}$  are orthogonal standard normal random variables, i.e.,  $\langle \xi_i \xi_j \rangle = \delta_{ij}$ ,  $f_i(\mathbf{x})$  and  $\alpha_i(\mathbf{x})$  can be determined separately from (10) with the corresponding covariance functions. Recalling (5), (8)–(10), and the definition of the Karhunen–Loeve expansion of a random space function, it can be seen that the deterministic functions  $f_i(\mathbf{x})$  and  $\alpha_i(\mathbf{x})$  in (22) are, respectively, proportional to  $\sigma_f$  and  $\sigma_\alpha$ , the standard deviations of the random functions  $f(\mathbf{x})$  and  $\alpha(\mathbf{x})$ .

By substituting (22) into (17)–(21), we have

$$Y^{(1)} = \sum_{i=1}^{\infty} Y_i \xi_i, \quad Y^{(2)} = \sum_{i,j=1}^{\infty} Y_{ij} \xi_i \xi_j \quad (23)$$

$$C^{(1)} = \sum_{i=1}^{\infty} C_i \xi_i, \quad C^{(2)} = \sum_{i,j=1}^{\infty} C_{ij} \xi_i \xi_j \quad (24)$$

$$q^{(1)} = \sum_{i=1}^{\infty} q_i \xi_i, \quad q^{(2)} = \sum_{i,j=1}^{\infty} q_{ij} \xi_i \xi_j \quad (25)$$

$$p^{(1)} = \sum_{i=1}^{\infty} p_i \xi_i, \quad p^{(2)} = \sum_{i,j=1}^{\infty} p_{ij} \xi_i \xi_j \quad (26)$$

The quantities in the summations of (23)–(26) are defined in Appendix A.

#### 4.2. Uncorrelated $f(\mathbf{x})$ and $\alpha(\mathbf{x})$

For the uncorrelated case,  $f(\mathbf{x})$  and  $\alpha(\mathbf{x})$  can be decomposed by two sets of independent orthogonal

normal random variables in the Karhunen–Loeve expansion as

$$\begin{aligned} f^l(\mathbf{x}) &= \sum_{i=1}^{\infty} f_i(\mathbf{x})\xi_i(\omega) \\ \alpha^l(\mathbf{x}) &= \sum_{i=1}^{\infty} \alpha_i(\mathbf{x})\eta_i(\omega) \end{aligned} \quad (27)$$

We have  $\langle \xi_i \eta_j \rangle = 0$  because  $\xi_i$  and  $\eta_i$  are uncorrelated normal variables and are thus independent.

Similarly to the perfectly correlated cases, substituting (27) into (17)–(21) leads to

$$Y^{(1)} = \sum_{i=1}^{\infty} Y_i^\xi \xi_i + \sum_{j=1}^{\infty} Y_j^\eta \eta_j, \quad (28)$$

$$Y^{(2)} = \sum_{i,j=1}^{\infty} Y_{ij}^{\xi\xi} \xi_i \xi_j + \sum_{i,j=1}^{\infty} Y_{ij}^{\xi\eta} \xi_i \eta_j + \sum_{i,j=1}^{\infty} Y_{ij}^{\eta\eta} \eta_i \eta_j$$

$$C^{(1)} = \sum_{i=1}^{\infty} C_i^\xi \xi_i + \sum_{j=1}^{\infty} C_j^\eta \eta_j, \quad (29)$$

$$C^{(2)} = \sum_{i,j=1}^{\infty} C_{ij}^{\xi\xi} \xi_i \xi_j + \sum_{i,j=1}^{\infty} C_{ij}^{\xi\eta} \xi_i \eta_j + \sum_{i,j=1}^{\infty} C_{ij}^{\eta\eta} \eta_i \eta_j$$

$$q^{(1)} = \sum_{i=1}^{\infty} q_i^\xi \xi_i + \sum_{j=1}^{\infty} q_j^\eta \eta_j, \quad (30)$$

$$q^{(2)} = \sum_{i,j=1}^{\infty} q_{ij}^{\xi\xi} \xi_i \xi_j + \sum_{i,j=1}^{\infty} q_{ij}^{\xi\eta} \xi_i \eta_j + \sum_{i,j=1}^{\infty} q_{ij}^{\eta\eta} \eta_i \eta_j$$

$$p^{(1)} = \sum_{i=1}^{\infty} p_i^\xi \xi_i + \sum_{j=1}^{\infty} p_j^\eta \eta_j, \quad (31)$$

$$p^{(2)} = \sum_{i,j=1}^{\infty} p_{ij}^{\xi\xi} \xi_i \xi_j + \sum_{i,j=1}^{\infty} p_{ij}^{\xi\eta} \xi_i \eta_j + \sum_{i,j=1}^{\infty} p_{ij}^{\eta\eta} \eta_i \eta_j$$

The quantities in the summations of (28)–(31) are defined in Appendix B.

### 5. Perturbation equations

By substituting (14) into (1) and (2) and rearranging, we obtain

$$C(\mathbf{x}, t)e^{-Y(\mathbf{x}, t)} \frac{\partial h(\mathbf{x}, t)}{\partial t} = \nabla^2 h(\mathbf{x}, t) + \nabla Y(\mathbf{x}, t) \cdot \nabla [h(\mathbf{x}, t) + z] + g(\mathbf{x}, t)e^{-Y(\mathbf{x}, t)} \quad (32)$$

$$\{e^{Y(\mathbf{x}, t)} \nabla [h(\mathbf{x}, t) + z] \cdot \mathbf{n}(\mathbf{x})\}|_{\Gamma_2} = -Q_n(\mathbf{x}, t)$$

$$h(\mathbf{x}, t)|_{\Gamma_1} = h_{\Gamma_1}(\mathbf{x}, t)$$

$$h(\mathbf{x}, t)|_{t=0} = h_{\text{ini}}(\mathbf{x})$$

The pressure head  $h(\mathbf{x}, t)$  is a random function because it depends on the randomness of the input soil parameters  $f(\mathbf{x})$  and  $\alpha(\mathbf{x})$ . As shown earlier, we may express soil parameters and head-related quantities  $C(\mathbf{x}, t)$ ,  $Y(\mathbf{x}, t)$ ,  $e^{-Y(\mathbf{x}, t)}$ ,  $e^{Y(\mathbf{x}, t)}$  and  $h(\mathbf{x}, t)$  as infinite series  $C(\mathbf{x}, t) = C^{(0)} + C^{(1)} + C^{(2)} + \dots$ ,  $Y(\mathbf{x}, t) = Y^{(0)} + Y^{(1)} + Y^{(2)} + \dots$ ,  $e^{-Y} = \exp[-Y^{(0)}] \times [q^{(0)} + q^{(1)} + q^{(2)} + \dots]$ ,  $e^Y = \exp[-Y^{(0)}][p^{(0)} + p^{(1)} + p^{(2)} + \dots]$ , and  $h(\mathbf{x}, t) = h^{(0)} + h^{(1)} + h^{(2)} + \dots$ , with each term of  $C^{(i)}$ ,  $Y^{(i)}$ ,  $q^{(i)}$ ,  $p^{(i)}$ , and  $h^{(i)}$  proportional to the  $i$ th order of the standard deviation of  $f(\mathbf{x})$  and  $\alpha(\mathbf{x})$ . For simplicity, we drop function arguments  $(\mathbf{x}, t)$  in functions  $C(\mathbf{x}, t)$ ,  $Y(\mathbf{x}, t)$ ,  $e^{-Y(\mathbf{x}, t)}$ ,  $e^{Y(\mathbf{x}, t)}$  and  $h(\mathbf{x}, t)$  when this does not cause any confusion. By substituting these expressions into (32) and collecting terms at the same order, we have the following equation for the order  $m \geq 0$

$$\sum_{k=0}^m \sum_{l=0}^{m-k} \left[ e^{-Y^{(0)}} C^{(k)} q^{(l)} \frac{\partial h^{(m-k-l)}}{\partial t} \right] = \nabla^2 h^{(m)} + \sum_{k=0}^m \nabla Y^{(k)} \cdot \nabla [h^{(m-k)} + z \delta_{m-k,0}] + g e^{-Y^{(0)}} q^{(m)} \quad (33)$$

$$\sum_{k=0}^m \left[ e^{-Y^{(0)}} p^{(k)} \nabla (h^{(m-k)} + z \delta_{m-k,0}) \right] \cdot \mathbf{n}|_{\Gamma_2} = -Q_n \delta_{m,0}$$

$$h^{(m)}|_{\Gamma_1} = h_{\Gamma_1} \delta_{m,0}$$

$$h^{(m)}|_{t=0} = h_{\text{ini}} \delta_{m,0}$$

where  $\delta_{m,0}$  is the Kronecker delta function with  $\delta_{m,0} = 1$  for  $m = 0$  and  $\delta_{m,0} = 0$  for any other  $m$ .

Eq. (33) can be further simplified as

$$c_o \frac{\partial h^{(m)}}{\partial t} = \nabla^2 h^{(m)} + \nabla Y^{(0)} \cdot \nabla h^{(m)} + g^{(m)} \quad (34)$$

$$[\nabla h^{(m)} \cdot \mathbf{n}]|_{\Gamma_2} = Q^{(m)}$$

$$h^{(m)}|_{\Gamma_1} = h_{\Gamma_1}^{(m)}$$

$$h^{(m)}|_{t=0} = h_{\text{ini}}^{(m)}$$

$$c_o = e^{-Y^{(0)}} C^{(0)} q^{(0)}$$

It is worthwhile to note that the perturbation equations for different orders have the same form except for the driving terms  $g^{(m)}$ ,  $Q^{(m)}$ ,  $h_{\Gamma_1}^{(m)}$ , and  $h_{\text{ini}}^{(m)}$ . This property will make the numerical computation more efficient because it is not necessary to determine the basic matrix in each time step for different order terms. The driving terms  $g^{(m)}$ ,  $Q^{(m)}$ ,  $h_{\Gamma_1}^{(m)}$ , and  $h_{\text{ini}}^{(m)}$  are given in Appendix C.

### 6. Karhunen-Loeve and polynomial chaos based perturbation equations

In this section the perturbation equations of stochastic saturated–unsaturated water flow and the corresponding initial and boundary conditions are formulated by expressing the constitutive relationship of the soil parameters in the Karhunen-Loeve expansion and the pressure head in polynomial chaos expression, and combining with the perturbation method.

#### 6.1. Perfectly correlated $f(\mathbf{x})$ and $\alpha(\mathbf{x})$

The quantities  $C^{(i)}$ ,  $Y^{(i)}$ ,  $q^{(i)}$ ,  $p^{(i)}$ , which are related to the input random soil properties  $f(\mathbf{x})$  and  $\alpha(\mathbf{x})$ , are expressed by (23)–(26). The pressure head is expressed by polynomial chaos in (13) where the normal random variables  $\{\zeta_i\} = \{\xi_i\}$  for the perfectly correlated case. We assume

$$h^{(1)} = \sum_{i=1}^{\infty} h_i(\mathbf{x}, t) \xi_i, \quad h^{(2)} = \sum_{i,j=1}^{\infty} h_{ij}(\mathbf{x}, t) \xi_i \xi_j, \quad (35)$$

where  $h_i(\mathbf{x}, t)$  and  $h_{ij}(\mathbf{x}, t)$  are deterministic functions to be determined. Once  $h_i(\mathbf{x}, t)$ ,  $h_{ij}(\mathbf{x}, t)$ ,  $i, j = 1, 2, \dots$ , and  $h^{(0)}(\mathbf{x}, t)$  are obtained, the random representation of pressure head  $h(\mathbf{x}, t)$  can be determined to

the second order of  $\sigma_f$  and  $\sigma_\alpha$ . The moments of pressure head and water content can also be derived directly from the random representation of pressure head.

By substituting (16)–(26) into (34) for  $m = 1$ , multiplying the resulting equations by  $\xi_j$ ,  $j = 1, 2, \dots$ , taking expectation, and recalling that  $\langle \xi_i \xi_j \rangle = \delta_{ij}$ , we have

$$c_o \frac{\partial h_i}{\partial t} = \nabla^2 h_i + \nabla Y^{(0)} \cdot \nabla h_i + g_i \quad i = 1, 2, 3, \dots \quad (36)$$

$$[\nabla h_i \cdot \mathbf{n}]|_{\Gamma_2} = Q_i$$

$$h_i|_{\Gamma_1} = 0$$

$$h_i|_{t=0} = 0$$

$$Q_i = \{ - [p_i^{(1)} \nabla(h^{(0)} + z)] \cdot \mathbf{n} \}|_{\Gamma_2} / p^{(0)}$$

$$g_i = g e^{-Y^{(0)}} q_i^{(1)} + \nabla Y_i^{(1)} \cdot \nabla(h^{(0)} + z) - e^{-Y^{(0)}} (C^{(0)} q_i^{(1)} + C_i^{(1)} q^{(0)}) \frac{\partial h^{(0)}}{\partial t}$$

Eq. (36) is linear because all terms in  $Q_i$  and  $g_i$  are linear function of  $h_i$ . More importantly, when Eq. (36) is rearranged by collecting the dependent variable  $h_i$  into the left-hand-side and leaving the driving terms on the right-hand-side, it can be shown that all the driving terms are proportional to the standard deviation of random input function  $f(\mathbf{x})$  and/or  $\alpha(\mathbf{x})$ , indicating that  $h_i(\mathbf{x}, t)$  is proportional to  $\sigma_f$  and/or  $\sigma_\alpha$ . This means that representation of the first and second order terms of pressure head in the form of (35) is reasonable.

Similarly, for  $m = 2$ , we have

$$c_o \frac{\partial h_{ij}}{\partial t} = \nabla^2 h_{ij} + \nabla Y^{(0)} \cdot \nabla h_{ij} + g_{ij}, \quad (37)$$

$$i, j = 1, 2, 3, \dots$$

$$[\nabla h_{ij}] \cdot \mathbf{n}|_{\Gamma_2} = Q_{ij}$$

$$h_{ij}|_{\Gamma_1} = 0$$

$$h_{ij}|_{t=0} = 0$$

$$Q_{ij} = \{ - [p_i^{(1)} \nabla h_j + p_j^{(2)} \nabla(h^{(0)} + z)] \cdot \mathbf{n} - [p_j^{(1)} \nabla h_i + p_j^{(2)} \nabla(h^{(0)} + z)] \cdot \mathbf{n} \}|_{\Gamma_2} / 2p^{(0)}$$

$$g_{ij} = g e^{-Y^{(0)}} q_{ij}^{(2)} + \nabla Y_i^{(1)} \cdot \nabla h_j + \nabla Y_{ij}^{(2)} \cdot \nabla(h^{(0)} + z) - e^{-Y^{(0)}} \left[ (C^{(0)} q_i^{(1)} + C_i^{(1)} q^{(0)}) \frac{\partial h_j}{\partial t} + (C^{(0)} q_{ij}^{(2)} + C_i^{(1)} q_j^{(1)} + C_{ij}^{(2)} q^{(0)}) \frac{\partial h^{(0)}}{\partial t} \right]$$

Note that although the zero order (34) and (C1) are nonlinear because the coefficient  $e$  and  $Y^{(0)}$  in Eq. (34) and Eq. (C1) depend on the dependent function  $h^{(0)}$ , Eqs. (36) and (37) are linear when those equations are solved sequentially. This property leads to numerical efficiency especially for the solution of the higher order terms in the polynomial chaos expression of the pressure head.

## 6.2. Uncorrelated $f(\mathbf{x})$ and $\alpha(\mathbf{x})$

The quantities  $C^{(i)}$ ,  $Y^{(i)}$ ,  $q^{(i)}$  and  $p^{(i)}$  are expressed by (28)–(31) from Karhunen-Loeve expansions. The polynomial chaos expression of pressure head in Eq. (13) can be expanded by two sets of uncorrelated normal random variables  $\{\xi_i\}$  and  $\{\eta_j\}$  as

$$h(\mathbf{x}, t) = h^{(0)} + h^{(1)} + h^{(2)} + \dots \quad (38)$$

$$h^{(1)} = \sum_{i=1}^{\infty} (h_i^\xi \xi_i + h_i^\eta \eta_i)$$

$$h^{(2)} = \sum_{i=1}^{\infty} \sum_{j=1}^{\infty} (h_{ij}^{\xi\xi} \xi_i \xi_j + h_{ij}^{\xi\eta} \xi_i \eta_j + h_{ij}^{\eta\eta} \eta_i \eta_j)$$

By substituting (28)–(31) and (38) into (34) for  $m = 1$  and Eq. (C2), multiplying  $\xi_j$  and  $\eta_j$ ,  $j = 1, 2, 3, \dots$ , taking expectation of the resulting equations, and considering the following properties of  $\xi_j$  and  $\eta_j$

$$\langle \xi_i \xi_j \rangle = \delta_{ij}, \quad \langle \eta_i \eta_j \rangle = \delta_{ij}, \quad \langle \xi_i \eta_j \rangle = 0$$

we obtain

$$c_o \frac{\partial h_i^\xi}{\partial t} = \nabla^2 h_i^\xi + \nabla Y^{(0)} \cdot \nabla h_i^\xi + g_i^\xi \quad i = 1, 2, 3, \dots \quad (39)$$

$$[\nabla h_i^\xi \cdot \mathbf{n}]|_{\Gamma_2} = Q_i^\xi$$

$$(h_i^\xi)|_{\Gamma_1} = 0$$

$$\begin{aligned} (h_i^\xi)|_{t=0} &= 0 \\ Q_i^\xi &= -[p_i^\xi \nabla(h^{(0)} + z) \cdot \mathbf{n}]|_{\Gamma_2}/p^{(0)} \\ g_i^\xi &= g e^{-Y^{(0)}} q_i^\xi + \nabla Y_i^\xi \cdot \nabla(h^{(0)} + z) \\ &\quad - e^{-Y^{(0)}} (C^{(0)} q_i^\xi + C_i^\xi q^{(0)}) \frac{\partial h^{(0)}}{\partial t} \end{aligned}$$

and

$$c_o \frac{\partial h_i^\eta}{\partial t} = \nabla^2 h_i^\eta + \nabla Y^{(0)} \cdot \nabla h_i^\eta + g_i^\eta \quad i = 1, 2, 3, \dots \quad (40)$$

$$\begin{aligned} [\nabla h_i^\eta \cdot \mathbf{n}]|_{\Gamma_2} &= Q_i^\eta \\ (h_i^\eta)|_{\Gamma_1} &= 0 \\ (h_i^\eta)|_{t=0} &= 0 \\ Q_i^\eta &= -[p_i^\eta \nabla(h^{(0)} + z) \cdot \mathbf{n}]|_{\Gamma_2}/p^{(0)} \\ g_i^\eta &= g e^{-Y^{(0)}} q_i^\eta + \nabla Y_i^\eta \cdot \nabla(h^{(0)} + z) \\ &\quad - e^{-Y^{(0)}} (C^{(0)} q_i^\eta + C_i^\eta q^{(0)}) \frac{\partial h^{(0)}}{\partial t} \end{aligned}$$

By substituting (28)–(31) and (38) into (34) for  $m = 2$  and Eq. (C3), we have

$$\begin{aligned} \sum_{i,j=1}^{\infty} L_{ij}^{\xi\xi} (h_i^{\xi\xi}) \xi_i \xi_j + \sum_{i,j=1}^{\infty} L_{ij}^{\xi\eta} (h_i^{\xi\eta}) \xi_i \eta_j \\ + \sum_{i,j=1}^{\infty} L_{ij}^{\eta\eta} (h_i^{\eta\eta}) \eta_i \eta_j = 0 \end{aligned} \quad (41)$$

where  $L_{ij}^{\xi\xi} (h_i^{\xi\xi})$ ,  $L_{ij}^{\xi\eta} (h_i^{\xi\eta})$ , and  $L_{ij}^{\eta\eta} (h_i^{\eta\eta})$  are defined in Appendix D.

Multiplying (41) by  $\xi_m \xi_n$  and  $\eta_m \eta_n$ ,  $m, n = 1, 2, \dots$ , considering the orthogonarity and the independency of series  $\{\xi_i\}$  and  $\{\eta_i\}$ , and taking expectation of the resulting equation yields

$$L_{mm}^{\xi\xi} (h_m^{\xi\xi}) + L_{mm}^{\eta\eta} (h_m^{\eta\eta}) = 0, \quad m, n = 1, 2, 3, \dots \quad (42)$$

$$L_{mm}^{\xi\eta} (h_m^{\xi\eta}) = 0$$

Eq. (42) can be further simplified as

$$c_o \frac{\partial h_{ij}}{\partial t} = \nabla^2 h_{ij} + \nabla Y^{(0)} \cdot \nabla h_{ij} + g_{ij}, \quad (43)$$

$$i \geq j = 1, 2, 3, \dots$$

$$[\nabla h_{ij} \cdot \mathbf{n}]|_{\Gamma_2} = Q_{ij}$$

$$h_{ij}|_{\Gamma_1} = 0$$

$$h_{ij}|_{t=0} = 0$$

where  $h_{ij} = h_{ij}^{\xi\xi} + h_{ij}^{\eta\eta}$ , and  $Q_{ij}$  and  $g_{ij}$  are defined in Appendix E.

Similar to the perfectly correlated case, the partial differential equations for the deterministic head coefficients  $h_i^\xi, h_i^\eta$  and  $h_{ij}$  are linear.

### 7. Means and variances of pressure head and water content

Once Eqs. (34), (36), (37), (39), (40), and (43) are solved, the mean and variance of pressure head can be computed directly. In this work, only second order terms of pressure head  $h(\mathbf{x}, t)$  is determined, all the moments are evaluated up to second order in the standard deviation of  $f(\mathbf{x})$  and  $\alpha(\mathbf{x})$ . The mean and variance of pressure head and water content are expressed as

$$\langle h(\mathbf{x}, t) \rangle = h^{(0)} + \sum_{i=1}^{\infty} (h_{ii}^{\xi\xi} + h_{ii}^{\eta\eta}), \quad (44)$$

$$\sigma_h^2 = \sum_{i=1}^{\infty} [(h_i^\xi)^2 + (h_i^\eta)^2]$$

$$\begin{aligned} \langle \theta \rangle &= (\theta_s - \theta_r) \exp\left(\frac{1}{2} \bar{\alpha} h^{(0)}\right) \left\{ \left(1 - \frac{1}{2} \alpha h\right) \right. \\ &\quad - \frac{1}{4} \bar{\alpha}^2 (h^{(0)})^2 \sum_{i=1}^{\infty} (h_{ii}^{\xi\xi} + h_{ii}^{\eta\eta}) \\ &\quad + \bar{\alpha}^2 \left(-\frac{1}{8} - \frac{1}{16} \bar{\alpha} h^{(0)}\right) \sum_{i=1}^{\infty} [(h_i^\xi)^2 + (h_i^\eta)^2] \\ &\quad + \bar{\alpha} h^{(0)} \left(-\frac{1}{2} - \frac{1}{8} \bar{\alpha} h^{(0)}\right) \sum_{i=1}^{\infty} \alpha_i h_i^\eta \\ &\quad \left. + (h^{(0)})^2 \left(-\frac{1}{8} - \frac{1}{16} \bar{\alpha} h^{(0)}\right) \sum_{i=1}^{\infty} \alpha_i \alpha_i \right\} \end{aligned} \quad (45)$$

$$\begin{aligned} \sigma_\theta^2 &= (\theta_s - \theta_r)^2 \exp(\bar{\alpha} h^{(0)}) \frac{1}{16} \bar{\alpha}^2 (h^{(0)})^2 \\ &\quad \times \left[ \bar{\alpha}^2 \sum_{i=1}^{\infty} (h_{ii}^{\xi\xi} + h_{ii}^{\eta\eta}) + 2 \bar{\alpha} h^{(0)} \sum_{i=1}^{\infty} \alpha_i h_i^\eta \right. \\ &\quad \left. + (h^{(0)})^2 \sum_{i=1}^{\infty} \alpha_i \alpha_i \right] \end{aligned}$$

for the case of uncorrelated  $f(\mathbf{x})$  and  $\alpha(\mathbf{x})$ , and

$$\langle h(\mathbf{x}, t) \rangle = h^{(0)} + \sum_{i=1}^{\infty} h_{ii} \quad (46)$$

$$\sigma_h^2 = \sum_{i=1}^{\infty} (h_i)^2$$

$$\begin{aligned} \langle \theta \rangle = & (\theta_s - \theta_t) \exp\left(\frac{1}{2} \bar{\alpha} h^{(0)}\right) \left\{ \left(1 - \frac{1}{2} \alpha h\right) \right. \\ & - \frac{1}{4} \bar{\alpha}^2 (h^{(0)})^2 \sum_{i=1}^{\infty} h_{ii} \\ & + \bar{\alpha}^2 \left(-\frac{1}{8} - \frac{1}{16} \bar{\alpha} h^{(0)}\right) \sum_{i=1}^{\infty} (h_i)^2 \\ & + \bar{\alpha} h^{(0)} \left(-\frac{1}{2} - \frac{1}{8} \bar{\alpha} h^{(0)}\right) \sum_{i=1}^{\infty} \alpha_i h_i \\ & \left. + (h^{(0)})^2 \left(-\frac{1}{8} - \frac{1}{16} \bar{\alpha} h^{(0)}\right) \sum_{i=1}^{\infty} \alpha_i \alpha_i \right\} \quad (47) \end{aligned}$$

$$\begin{aligned} \sigma_{\theta}^2 = & (\theta_s - \theta_t)^2 \exp(\bar{\alpha} h^{(0)}) \frac{1}{16} \bar{\alpha}^2 (h^{(0)})^2 \\ & \times \left[ \bar{\alpha}^2 \sum_{i=1}^{\infty} h_{ii} + 2 \bar{\alpha} h^{(0)} \sum_{i=1}^{\infty} \alpha_i h_i + (h^{(0)})^2 \sum_{i=1}^{\infty} \alpha_i \alpha_i \right] \end{aligned}$$

for the case of perfectly correlated  $f(\mathbf{x})$  and  $\alpha(\mathbf{x})$ .

## 8. Numerical implementation

The head coefficient (34), (36), (37), (39), (40), and (43) are deterministic partial differential equations and cannot, in general, be solved analytically and are therefore solved by any efficient and reader preferred numerical method. The numerical implementation is facilitated by recognizing that the head coefficients are governed by the same type of equations but with different forcing terms. We approximate the spatial derivatives by a central-difference scheme and the temporal derivatives by an implicit method. The zero order mean flow equation for both perfectly correlated and uncorrelated cases is the same. This equation is nonlinear and thus needs to be solved in an iterative manner. Once the mean pressure head  $h^{(0)}$  is solved, the linear equations for the other head coefficient terms can be solved sequentially and the coefficient matrix of the resulting system equations are the same.

This behavior of the resulting head coefficient equations renders efficiency in the numerical method.

Due to the symmetry of the coefficients  $h_{ij}(\mathbf{x}, t) \times (i, j = 1, 2, \dots, N_p)$ , the number of times needed to solve the linear system of equations is  $N_p(N_p + 1)/2$ , where  $N_p$  is the number of truncation terms of the Karhunen-Loeve expansion. Because up to second order terms are evaluated in this study, only  $h_{ii}(\mathbf{x}, t) \times (i = 1, 2, \dots, N_p)$  are needed for the calculation of the moment of pressure head and water content, which reduce the computational efforts significantly.

## 9. Illustrative examples

In this section we attempt to demonstrate the applicability of the developed stochastic model to saturated–unsaturated flow in hypothetical soils. The log-transformed saturated hydraulic conductivity  $f(\mathbf{x})$  and the pore size distribution parameter  $\alpha(\mathbf{x})$  are assumed to be second order stationary, with a separable exponential covariance given in (7). In this situation, the eigenvalues and eigenfunctions can be determined analytically by (8)–(11). Fig. 1 shows the monotonic decay of the eigenvalues. The decay rate is related to the correlation length and the size of the simulation domain. The larger the correlation length, the faster the decay rate of the eigenvalue to zero, and the fewer terms needed in the Karhunen-Loeve expansion. In the selected examples with

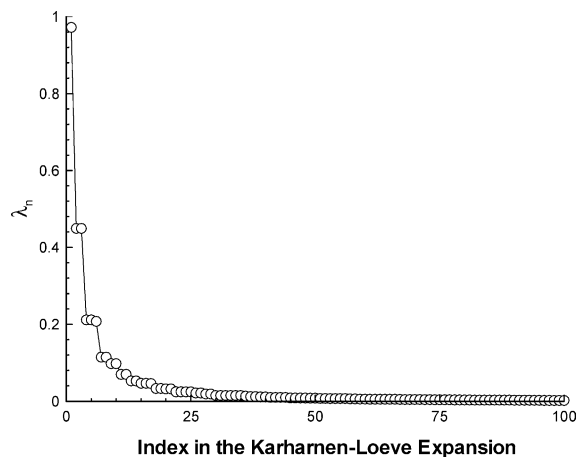


Fig. 1. Eigenvalues associated with Eq. (7) for  $\gamma_1 = \gamma_2 = 50$  cm and  $L_1 = L_2 = 150$  cm.

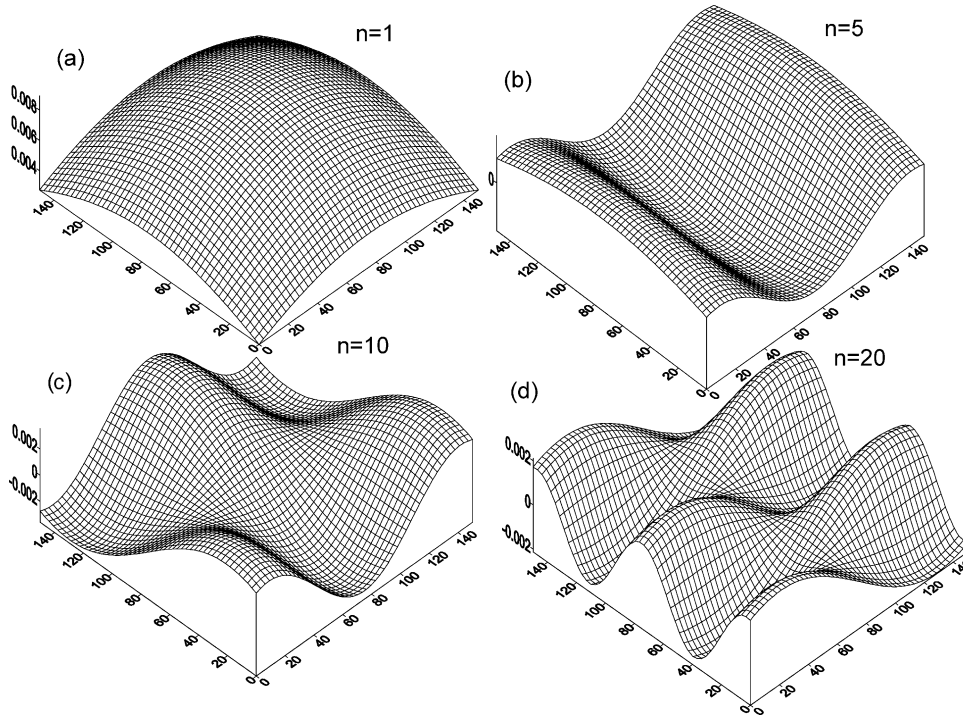


Fig. 2. Eigenfunctions  $\phi_i^*$  for  $n = 1, 5, 10$  and  $20$  associated with Eq. (9) for  $\gamma_1 = \gamma_2 = 50$  cm and  $L_1 = L_2 = 150$  cm.

the correlation length from 30 to 50 cm, only 10–80 terms are required to obtain results that are consistent with the first-order moment-based model. Fig. 2 shows some eigenfunctions obtained from Eq. (10). With the increase of the terms in the KL expansion, the higher frequency random fluctuations will be involved in the analysis, and the contribution of these higher frequency terms to the solution processes will decrease because the eigenvalues decrease dramatically.

The numerical approach can easily handle the nonstationarity if other forms of covariances of  $f(\mathbf{x})$  and  $\alpha(\mathbf{x})$  are provided and Eq. (6) can be solved analytically or numerically to determine the eigenvalues and eigenfunctions, which serve as the input to the numerical solution of the head coefficient equations.

### 9.1. Uncorrelated case

In this example, we first try to show the validity of the proposed stochastic models and numerical

implementation by comparing our numerical results with those from the conventional moment-equation-based stochastic models (Lu and Zhang, 2002; Zhang and Lu, 2002). We consider a rectangle grid of  $21 \times 61$  nodes in a vertical cross-section of  $120$  cm  $\times$   $360$  cm. The boundary conditions are specified as follows: constant pressure head at the bottom with the pressure  $h = 0$ , a constant infiltration flux  $Q_2$  at the top, and no-flow at the left and right sides. The input parameters are given as  $\bar{f} = 0.0$  (i.e. the geometric mean of saturated hydraulic conductivity equals to  $1.0$  cm/ $T$ , where  $T$  is any time unit, as long as it is consistent with the time unit in  $Q_2$ ),  $\sigma_f^2 = 0.1$ ,  $\bar{\alpha} = 0.03$  cm $^{-1}$ ,  $\sigma_\alpha^2 = 2.5 \times 10^{-5}$  cm $^{-2}$ ,  $\gamma_{fx} = \gamma_{fz} = \gamma_{\alpha x} = \gamma_{\alpha z} = 30$  cm,  $\theta_s = 0.3$ ,  $\theta_r = 0.0$ ,  $Q_2 = -0.01$  cm/ $T$ , where negative sign in  $Q_2$  represents infiltration. Fig. 3 depicts the first two moments of pressure head at the steady state from the Karhunen-Loeve expansion and perturbation based stochastic model (KL-based model) and the moment-equation-based stochastic model (moment-based model). The zeroth-order mean equations are

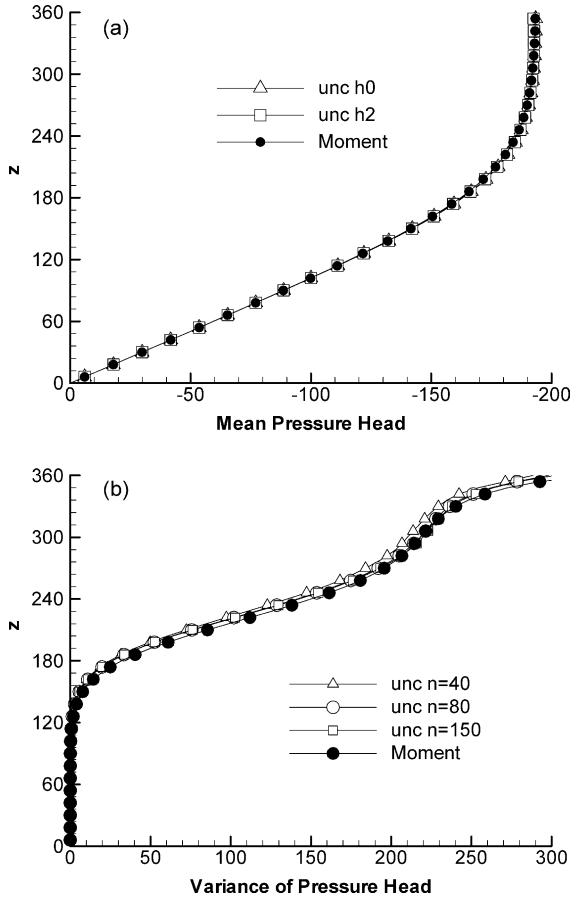


Fig. 3. Comparison of the mean pressure head and variance calculated from the KL-based model with those from moment-based model, the uncorrelated case. ‘unc’ indicates uncorrelated  $f(\mathbf{x})$  and  $\alpha(\mathbf{x})$ .

the same from the two stochastic models. In the KL-based model the second-order mean pressure head is calculated and it is shown that the contribution of the second-order terms to the mean pressure head is small for the given statistical parameters of the random functions (Fig. 3a). We also calculated the mean pressure head to second order for the case  $\sigma_f^2 = 0.5$ ,  $\sigma_\alpha^2 = 2.0 \times 10^{-4} \text{ cm}^{-2}$ , and  $\gamma_{fx} = \gamma_{fz} = \gamma_{\alpha x} = \gamma_{\alpha z} = 30 \text{ cm}$ , and obtained a similar result. Fig. 3b shows the variance of pressure head from the moment-based model and that from the KL-based model with different numbers of terms in the Karhunen-Loeve expansions of  $f(\mathbf{x})$  and  $\alpha(\mathbf{x})$ . When we expand  $f(\mathbf{x})$  and  $\alpha(\mathbf{x})$  with 80 terms, the pressure head variance from the two stochastic models

are almost the same. This comparison indicates the correctness of our proposed model, because the moment-based model has been validated previously by Monte Carlo simulations (Zhang and Lu, 2002). More importantly, this example demonstrates the efficiency of the proposed model in computational efforts compared with the moment-based model, at least for the random parameters given in these examples. In the moment-based model, equations for  $C_{hh}(\mathbf{x}, \mathbf{y}; t, \tau)$ ,  $C_{hf}(\mathbf{x}, \mathbf{y}; t, \tau)$ ,  $C_{h\alpha}(\mathbf{x}, \mathbf{y}; t, \tau)$  and the mean equation of pressure head have to be solved (Zhang and Lu, 2002). Because the covariance equations are functions of arbitrary two space points  $\mathbf{x}$  and  $\mathbf{y}$  in the simulation domain, the computation of these equations is demanding. Instead of solving the covariance equations, the KL-based model solves for a small number of the deterministic coefficients  $h_i(\mathbf{x}, t)$  and  $h_{ii}(\mathbf{x}, t)$ ,  $i = 1, 2, \dots, N_p$ , which are governed by the equations that are similar to the covariance equations (with fixed reference point  $\mathbf{y}$ ) in the moment-based model, where  $N_p$  is the number of terms in KL-expansion of the random function  $f(\mathbf{x})$  and  $\alpha(\mathbf{x})$ . For the case of  $n$  grid nodes in the simulation domain, the moment-based model needs to solve the resultant linear system of equations for  $n_m = n_i + 3 \times n$  times, where  $n_i$  is the number of iterations for the nonlinear equation of mean pressure head. The KL-based model needs to solve the equations for  $n_k = n_i + 3 \times N_p$  times. In the present example,  $n = 1271$ ,  $N_p = 80$ , and  $n_i = 6$ , we have  $n_m = 3819$  and  $n_k = 246$ , giving approximately a difference of 15 times between the two models. This advantage will be more significant for larger-size problems and for the higher-order analysis (Zhang and Lu, 2004).

## 9.2. Perfectly correlated case

Since the moment-based computer model of Zhang and Lu (2002) did not implement the perfectly correlated case, we first conduct simplified simulations to test the correctness of the proposed perfectly correlated KL-based model. We assume that one of the variances of  $f(\mathbf{x})$  and  $\alpha(\mathbf{x})$  equals to zero and compare the simulation results with those from the corresponding moment-based model. One simulation case is for the input variance  $\sigma_\alpha^2 = 0$  and  $\sigma_f^2 = 2.0$  and another case for  $\sigma_\alpha^2 = 2.0 \times 10^{-4}$  and  $\sigma_f^2 = 0$ . All other input parameters for the two cases

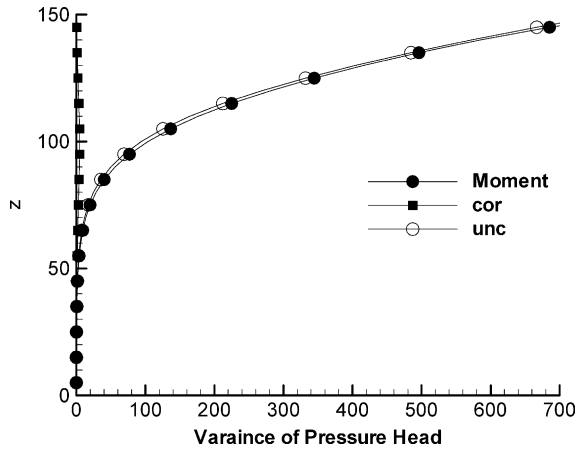


Fig. 4. Calculated pressure head variance from the KL-based model of the perfectly correlated and uncorrelated cases and compared with that from the moment-based model.  $\sigma_f^2 = 2$ ,  $\sigma_\alpha^2 = 2.0 \times 10^{-4}$ ,  $\gamma_{fx} = \gamma_{fz} = \gamma_{\alpha x} = \gamma_{\alpha z} = 50$  cm,  $L_1 = L_2 = 150$  cm. ‘unc’ indicates uncorrelated case and cor indicates perfectly correlated case.

are the same:  $\bar{\alpha} = 0.04 \text{ cm}^{-1}$ ,  $\gamma_{fx} = \gamma_{fz} = \gamma_{\alpha x} = \gamma_{\alpha z} = 50$  cm,  $L_1 = L_2 = 150$  cm,  $\theta_s = 0.3$ ,  $\theta_r = 0.0$ , and  $Q_2 = -0.01 \text{ cm/T}$ . The simulation results from the KL-based models with different terms in the Karhunen-Loeve expansion both for perfectly correlated and uncorrelated cases are comparable with those from the moment-based model, indicating the correctness of model for these special cases.

Fig. 4 shows the effect of the correlation patterns of the input random functions on the pressure head variance. By using the same input random parameters as described above ( $\sigma_f^2 = 2.0$ ,  $\sigma_\alpha^2 = 2.0 \times 10^{-4} \text{ cm}^{-2}$ ), for uncorrelated case the head variance from the KL-based model and the moment-based model are identical. However, the head variance for the perfectly correlated case is significantly different from that for the uncorrelated case (Fig. 4). We compared our numerical results with the analytical solution of Yeh et al. (1985b) for both perfectly correlated and uncorrelated cases. From their analytical results, we can calculate the ratio  $r_{uc}$  of the standard deviation of the uncorrelated case to the perfectly correlated case,  $r_{uc} = (\sigma_h)_{unc}/(\sigma_h)_{cor} = (\sigma_f^2 + H_u^2 \sigma_\alpha^2)^{1/2}/(\sigma_f - H_c \sigma_\alpha)$ , where  $(\sigma_h)_{unc}$  and  $(\sigma_h)_{cor}$  are the standard deviation of pressure head,  $H_u$  and  $H_c$  are the suction head for the uncorrelated and correlated cases in unbounded domain, respectively. By substituting  $\sigma_f^2 = 2.0$ ,  $\sigma_\alpha^2 = 2.0 \times 10^{-4} \text{ cm}^{-2}$ ,

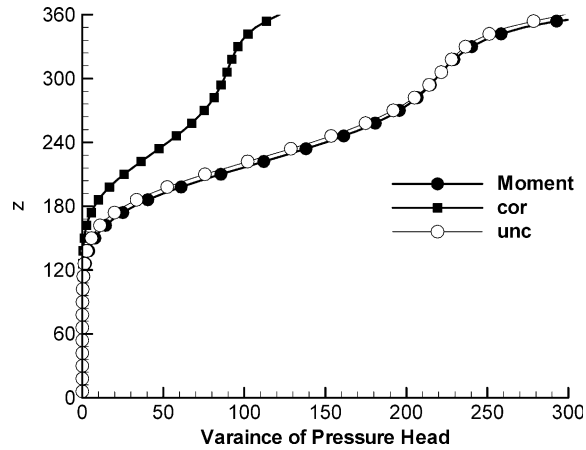


Fig. 5. Calculated pressure head variance from the KL-based model of the perfectly correlated and uncorrelated cases, and compared with that from the moment-based model.  $\sigma_f^2 = 0.1$ ,  $\sigma_\alpha^2 = 2.5 \times 10^{-5} \text{ cm}^{-2}$ ,  $\gamma_{fx} = \gamma_{fz} = \gamma_{\alpha x} = \gamma_{\alpha z} = 30$  cm,  $L_1 = 120$  cm,  $L_2 = 360$  cm.

and  $H_u = H_c = 109$  cm into above formula, we have  $r_{uc} = 11.2$ . The numerical result from the KL-based model in bounded domain for perfectly correlated and uncorrelated case is  $r_{uc} = 14.2$ , which is compatible with the analytical result of Yeh et al. (1985b) for unbounded domain. Fig. 5 presents the variance of pressure head for the case of perfectly correlated  $f(\mathbf{x})$  and  $\alpha(\mathbf{x})$ , the parameters of which are the same case as those for Fig. 3. It is seen that the inclusion of the  $f(\mathbf{x})$  and  $\alpha(\mathbf{x})$  correlation generally reduces the head variance. By substituting the simulation input parameters  $\sigma_f^2 = 0.1$ ,  $\sigma_\alpha^2 = 2.5 \times 10^{-5} \text{ cm}^{-2}$ , and  $H_u = H_c = 193$  cm, we have  $r_{uc} = 1.59$  from the analytical result of Yeh et al. (1985). In our example, the standard deviations of pressure head for uncorrelated and correlated cases are 17.3 and 11 cm, respectively, and we have  $r_{uc} = 1.60$ , which is very close to the result from the analytical model. Both our numerical results and the analytical results of Yeh et al. (1985) indicate that the correlation structures of  $f(\mathbf{x})$  and  $\alpha(\mathbf{x})$  have a large effect on the variance of pressure head.

### 9.3. Underground irrigation and drainage in saturated–unsaturated soils

The examples in this section show an underground pipe irrigation and a drainage problem in stationary

or nonstationary soils. In the example of underground pipe irrigation, the domain is of size  $150 \text{ cm} \times 150 \text{ cm}$ . The pipe is located at the depth of 50 cm below the ground surface with an irrigation rate of  $-0.1 \text{ cm}/T$ . The boundary conditions are: specified recharge ( $-0.01 \text{ cm}/T$ ) at the top and constant pressure head (0 cm) at the bottom, and no-flow boundaries at the two lateral sides. The input parameters are:  $\sigma_f^2 = 2.0$ ,  $\bar{\alpha} = 0.04 \text{ cm}^{-1}$ ,  $\sigma_\alpha^2 = 2.0 \times 10^{-4} \text{ cm}^{-2}$ ,  $\eta_{fx} = \eta_{fz} = \eta_{\alpha x} = \eta_{\alpha z} = 50 \text{ cm}$ ,  $\theta_s = 0.3$ , and  $\theta_r = 0.0$ . Fig. 6 illustrates the redistribution of irrigated water and the corresponding standard deviations of pressure head and water content in the domain. When water is irrigated from the underground

pipe, pressure head near the pipe is higher and so is the mean water content (Fig. 6a and b). However, the standard deviations of pressure head and water content have different patterns. Near the irrigation pipe, the pressure head standard deviation is high compared to that in the surrounding area, but the standard deviation of water content is lower near the pipe. This is reasonable because the standard deviation of water content becomes small when the water content increases with the increasing pressure. In the practical experience, the water content variability of samples from the very dry or very wet soil is small and the large water content variability is always found in the middle range of water content. Fig. 7 shows the effect of

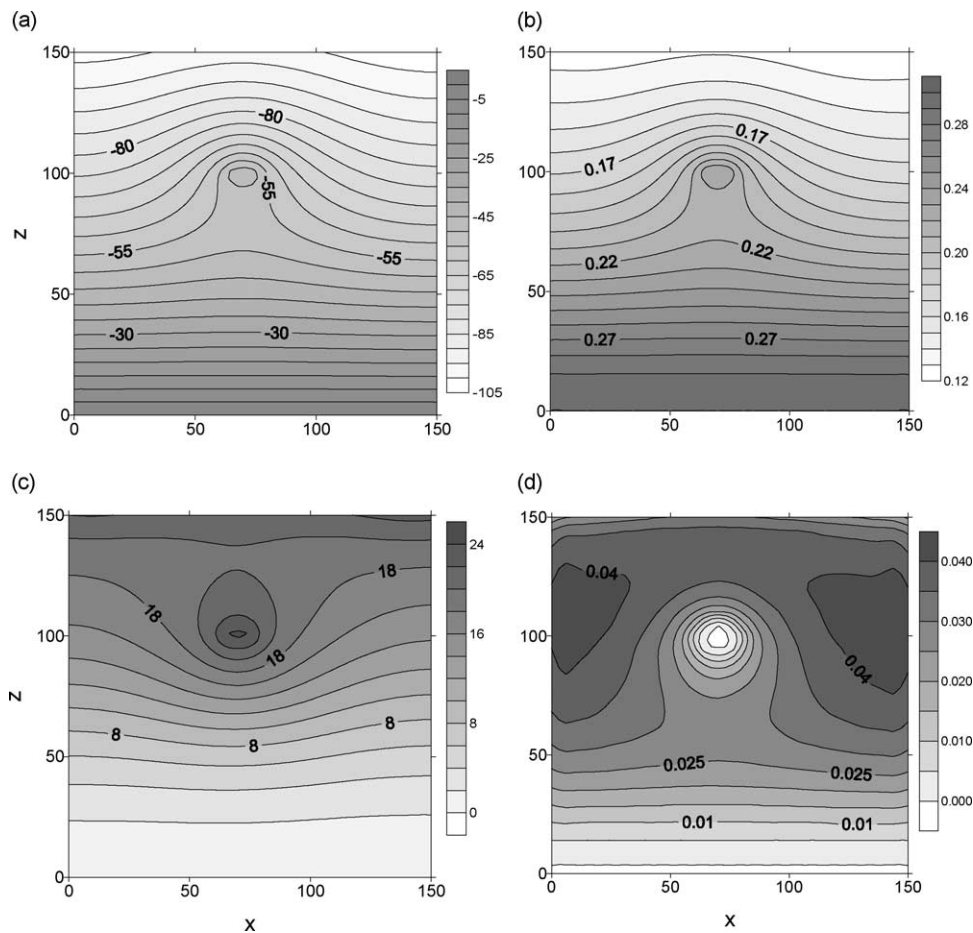


Fig. 6. Contours of mean (a) and standard deviation (c) of pressure head, and mean (b) and standard deviation (d) of water content for the cases with pipe irrigation.

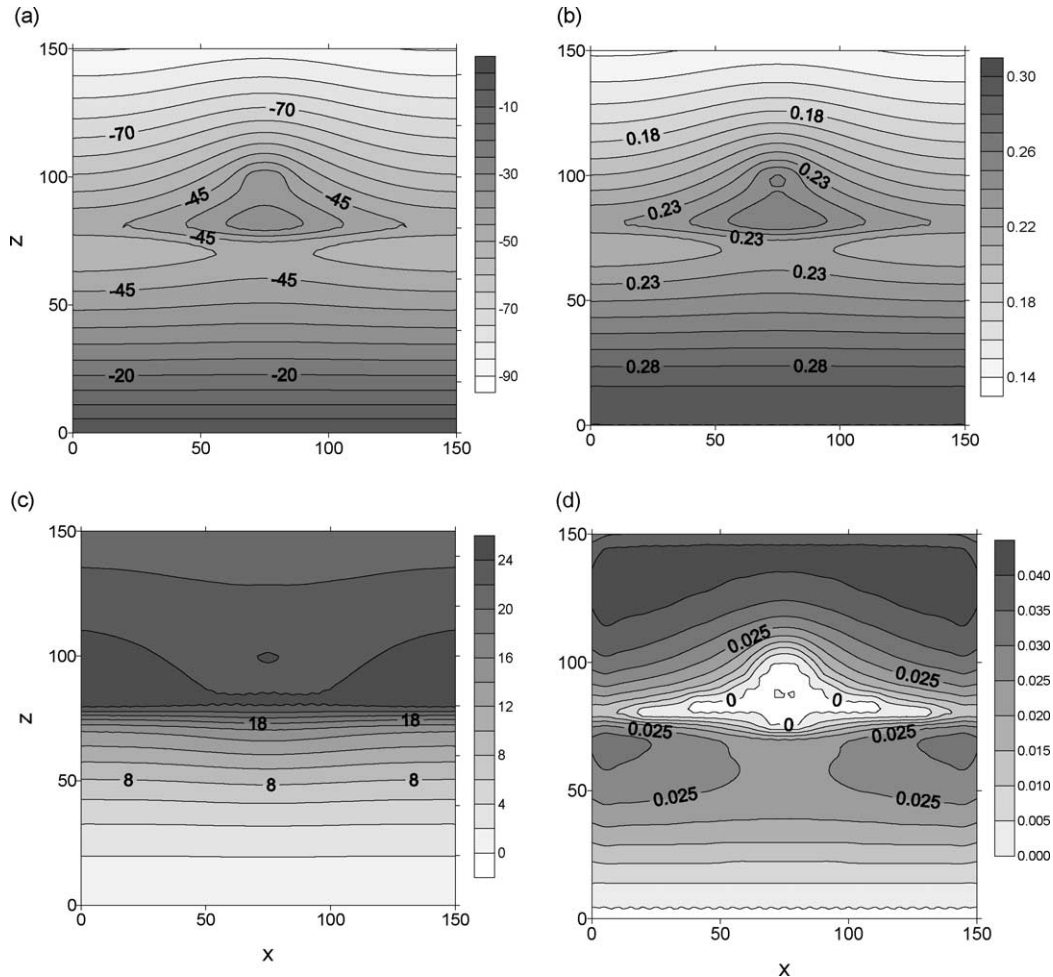


Fig. 7. Contours of mean (a) and standard deviation (c) of pressure head, and mean (b) and standard deviation (d) of water content for the cases with pipe irrigation and an embedded zone of lower mean saturated conductivity below the irrigation pipe.

medium nonstationary on statistics of the soil water distribution. In this example, there is a thin layer of slightly different soils embedded in the otherwise spatially stationary soil. The layer is of thickness 10 cm and width 150 cm with its center at depth of 65 cm below the ground surface. The geometric mean of saturated soil conductivity of the layer is 0.135 cm/T, and all other parameters are kept unchanged. Comparison between Fig. 7 and Fig. 6 reveals that this nonstationary medium feature has a significant impact on the mean pressure head field and the associated predictive uncertainty. The maximum standard

deviation of pressure head for the nonstationary  $f(\mathbf{x})$  distribution is along the top of the lower conductivity layer (Fig. 7c) and for the stationary one is near the irrigation pipe (Fig. 6c). Fig. 7b and d are also very different from their counterparts in Fig. 6 in that the soil water moves mainly in the lateral direction above the thin layer (Fig. 7b) while it moves preferentially downward for the case of stationary medium (Fig. 6b). The small water content standard deviation region is below the irrigation pipe and above the lower conductivity layer where the water content is large (Fig. 7d).

The next example involves flow to a drain in a saturated–unsaturated system with infiltration at the top, impermeable boundaries at the other three sides, and a drain in the middle of the left side. The drain is simulated as a constant pressure head boundary. The flow domain with a size of 600 cm in the horizontal direction and 300 cm in the vertical direction is divided into  $30 \times 60$  square elements. The soil properties are given as  $\sigma_f^2 = 0.5$ ,  $\bar{\alpha} = 0.03 \text{ cm}^{-1}$ ,  $\sigma_\alpha^2 = 2.5 \times 10^{-5} \text{ cm}^{-2}$ ,  $\eta_{fx} = \eta_{fz} = \eta_{\alpha x} = \eta_{\alpha z} = 50 \text{ cm}$ ,  $\theta_s = 0.3$ , and  $\theta_r = 0.0$ . The uniformly distributed infiltration rate at the surface is  $Q_1 = -0.01 \text{ cm/T}$ . The simulated mean and standard deviation of total hydraulic head, and water flow pattern are shown in Fig. 8. Because the head standard deviation is zero at the constant head boundary (i.e. at the drain), the maximum standard deviation occurs along the soil surface where the infiltration boundary is applied (Fig. 8a). In this unsaturated–saturated system, both the mean and the standard deviation of the flow quantities have complicated, nonstationary patterns, which cannot

be delineated accurately without considering the coupling between the two flow regimes.

## 10. Summary and conclusions

A stochastic model for transient flow in saturated–unsaturated zones is developed based on the Karhunen-Loeve expansion of the input random functions combined with the perturbation method. The log-transformed saturated hydraulic conductivity  $f(\mathbf{x})$  and the soil pore size distribution parameter  $\alpha(\mathbf{x})$  are assumed to be normal random functions with known covariances.  $f(\mathbf{x})$  and  $\alpha(\mathbf{x})$  are first expanded by the Karhunen-Loeve decomposition and the pressure head is expanded as polynomial chaos with the same set of random variables as those from the expansion of  $f(\mathbf{x})$  and  $\alpha(\mathbf{x})$ . We studied the cases of perfectly correlated or uncorrelated  $f(\mathbf{x})$  and  $\alpha(\mathbf{x})$ . By using the Karhunen-Loeve expansion of the input random parameters, polynomial chaos expansion of pressure head, and the perturbation method, the governing equation of the saturated–unsaturated flow and the corresponding initial and boundary conditions are represented by a series of partial differential equations in which the dependent variables are deterministic coefficients of the polynomial chaos expansion. Once the partial differential equations are solved subsequently, the deterministic coefficients in the polynomial chaos expansion are obtained and the random representation of the pressure head is obtained by combining these deterministic coefficients and the random variables from the Karhunen-Loeve expansion of the input random functions through truncated polynomial expansions. The moments of pressure head and water content can be determined efficiently by taking the advantage of the orthogonality of the normal random variables in the expansion. We demonstrated applicability of the proposed KL-based stochastic model with some examples of unsaturated and saturated–unsaturated flow in two dimensions and compared the results with those by the moment-based stochastic model. The main findings of this paper are as follows:

1. By combining the Karhunen-Loeve expansion of the input random function of the unsaturated

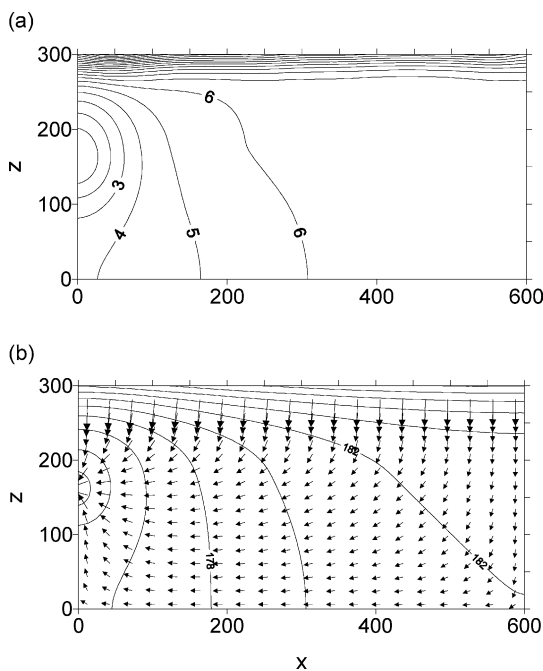


Fig. 8. Contours of standard deviation of pressure head (a), and total hydraulic head and flow field (b) with the drainage in saturated–unsaturated soils.

porous media  $f(\mathbf{x})$  and  $\alpha(\mathbf{x})$ , the polynomial chaos expansion of pressure head  $h(\mathbf{x}, t)$ , and the perturbation method, the governing equation of the saturated–unsaturated flow and the initial and boundary conditions can be represented by a series of partial differential equations which can be solved by any suitable numerical methods.

2. For the nonlinear saturated–unsaturated flow, only the zero order head equation is nonlinear, the other equations are linear. All the head coefficient equations of the same type but with different forcing terms, which will make the numerical modeling very effective because it is not necessary to rebuild the coefficient matrix for different orders of head coefficient equations in each time steps.
3. The developed KL-based stochastic models are compared with the moment-based stochastic model. The simulation results from the two stochastic models are identical for the same perturbation order. However, the proposed KL-based model is much more efficient because only a few terms in KL expansion are required (20–80 terms in our examples) for the input random porous media properties.
4. The illustrative examples show the potential applicability of the proposed stochastic model to the complicated saturated–unsaturated cases. The examples indicate that the correlation structures and the nonstationarity of the input random functions  $f(\mathbf{x})$  and  $\alpha(\mathbf{x})$  have a large effect on the calculated results of the mean and variance of pressure head and water content.

### Acknowledgements

The first author gratefully acknowledges the financial support of the Chinese Scholarship Foundation for his visit to Los Alamos National Laboratory, USA. The work was partially supported by a DOE/NGOTP grant awarded to Los Alamos National Laboratory, which is operated by the University of California for the US Department of Energy.

### Appendix A

By substituting (13) and (22) into (16)–(21), and collecting the like terms, we have

$$\begin{aligned}
 Y_i &= f_i + \bar{\alpha}h_i + h^{(0)}\alpha_i, & Y_{ij} &= \bar{\alpha}h_{ij} + \alpha_i h_j \\
 C_{11}h_i + C_{12}\alpha_i, & & C_{ij} &= C_{21}h_{ij} + C_{22}h_i h_j \\
 & & & + C_{23}h_i \alpha_j + C_{24}\alpha_i \alpha_j \\
 Y_i^{(1)} &= f_i + \bar{\alpha}h_i + h^{(0)}\alpha_i, & p_{ij} &= Y_{ij} + \frac{1}{2}Y_i Y_j \\
 p_i &= Y_i, & q_{ij} &= -Y_{ij} + \frac{1}{2}Y_i Y_j \\
 q_i &= -Y_i^{(1)},
 \end{aligned}$$

### Appendix B

By substituting (13) and (27) into (16)–(21), and collecting the terms of the same kind, we obtain

$$\begin{aligned}
 Y_i^\xi &= \bar{\alpha}h_i^\xi + f_i, & Y_j^\eta &= \bar{\alpha}h_j^\eta + h^{(0)}\alpha_j \\
 Y_{ij}^{\xi\xi} &= \bar{\alpha}h_{ij}^{\xi\xi}, & Y_{ij}^{\xi\eta} &= \bar{\alpha}h_{ij}^{\xi\eta} + \alpha_j h_i^\xi, \\
 Y_{ij}^{\eta\eta} &= \bar{\alpha}h_{ij}^{\eta\eta} + \frac{1}{2}(\alpha_i h_j^\eta + \alpha_j h_i^\eta) \\
 C_i^\xi &= C_{11}h_i^\xi, & C_j^\eta &= C_{11}h_j^\eta + C_{12}\alpha_j, \\
 C_{ij}^{\xi\xi} &= C_{21}h_{ij}^{\xi\xi} + C_{22}h_i^\xi h_j^\xi, & C_{ij}^{\xi\eta} &= C_{21}h_{ij}^{\xi\eta} + C_{23}h_i^\xi \alpha_j, \\
 C_{ij}^{\eta\eta} &= C_{21}h_{ij}^{\eta\eta} + \frac{1}{2}C_{23}(h_i^\eta \alpha_j + h_j^\eta \alpha_i) + C_{24}\alpha_i \alpha_j \\
 q_i^\xi &= -\bar{\alpha}h_i^\xi - f, & q_j^\eta &= -\bar{\alpha}h_j^\eta - h^{(0)}\alpha_j \\
 q_{ij}^{\xi\xi} &= -\bar{\alpha}h_{ij}^{\xi\xi} + \frac{1}{2}Y_i^\xi Y_j^\xi, & q_{ij}^{\xi\eta} &= -\bar{\alpha}h_{ij}^{\xi\eta} - \alpha_j h_i^\xi + Y_i^\xi Y_j^\eta \\
 q_{ij}^{\eta\eta} &= -\bar{\alpha}h_{ij}^{\eta\eta} - \frac{1}{2}(\alpha_i h_j^\eta + \alpha_j h_i^\eta) + \frac{1}{2}Y_i^\eta Y_j^\eta \\
 p_i^\xi &= \bar{\alpha}h_i^\xi + f, & p_j^\eta &= \bar{\alpha}h_j^\eta + h^{(0)}\alpha_j \\
 p_{ij}^{\xi\xi} &= \bar{\alpha}h_{ij}^{\xi\xi} + \frac{1}{2}Y_i^\xi Y_j^\xi, & p_{ij}^{\xi\eta} &= \bar{\alpha}h_{ij}^{\xi\eta} + \alpha_j h_i^\xi + Y_i^\xi Y_j^\eta \\
 p_{ij}^{\eta\eta} &= \bar{\alpha}h_{ij}^{\eta\eta} + \frac{1}{2}(\alpha_i h_j^\eta + \alpha_j h_i^\eta) + \frac{1}{2}Y_i^\eta Y_j^\eta
 \end{aligned}$$

### Appendix C

The driving terms  $g^{(m)}$ ,  $Q^{(m)}$ ,  $h_{\Gamma_1}^{(m)}$ , and  $h_{\text{ini}}^{(m)}$  can be determined from (33) for  $m = 1, 2$ , and  $3$ , respectively.

For  $m = 0$ , the driving terms are:

$$g^{(0)} = g e^{-Y^{(0)}} e n^{(0)} + \frac{\partial Y^{(0)}}{\partial z} \quad (\text{C1})$$

$$Q^{(0)} = -e^{-Y^{(0)}} Q_n / e p^{(0)} - \nabla_z \mathbf{n}$$

$$h_{\Gamma_1}^{(0)} = h_{\Gamma_1}, \quad h_{\text{ini}}^{(0)} = h_{\text{ini}}$$

For  $m = 1$ , we have

$$g^{(1)} = g e^{-Y^{(0)}} q^{(1)} + \nabla Y^{(1)} \cdot \nabla (h^{(0)} + z) - e^{-Y^{(0)}} (C^{(0)} q^{(1)} + C^{(1)} q^{(0)}) \frac{\partial h^{(0)}}{\partial t} \quad (\text{C2})$$

$$Q^{(1)} = \{ - [p^{(1)} \nabla (h^{(0)} + z)] \cdot \mathbf{n} \}_{\Gamma_2} / p^{(0)}$$

$$h_{\Gamma_1}^{(1)} = 0, \quad h_{\text{ini}}^{(1)} = 0$$

and for  $m = 2$ , we obtain

$$g^{(2)} = g e^{-Y^{(0)}} q^{(2)} + \nabla Y^{(1)} \cdot \nabla h^{(1)} + \nabla Y^{(2)} \cdot \nabla (h^{(0)} + z) - e^{-Y^{(0)}} \left[ (C^{(0)} q^{(1)} + C^{(1)} q^{(0)}) \frac{\partial h^{(1)}}{\partial t} + (C^{(1)} q^{(1)} + C^{(2)} q^{(0)} + C^{(0)} q^{(2)}) \frac{\partial h^{(0)}}{\partial t} \right] \quad (\text{C3})$$

$$Q^{(2)} = \{ - [p^{(1)} \nabla h^{(1)} + p^{(2)} \nabla (h^{(0)} + z)] \cdot \mathbf{n} \}_{\Gamma_2} / e p^{(0)}$$

$$h_{\Gamma_1}^{(2)} = 0, \quad h_{\text{ini}}^{(2)} = 0$$

### Appendix D

By substituting (27)–(31) and (38) into (C3) and collect the like terms which related to the uncorrelated normal random variables  $\xi_i$  and  $\eta_j$ , we have

$$\sum_{i,j=1}^{\infty} L_{ij}^{\xi\xi}(h^{\xi\xi}) \xi_i \xi_j + \sum_{i,j=1}^{\infty} L_{ij}^{\xi\eta}(h^{\xi\eta}) \xi_i \eta_j + \sum_{i,j=1}^{\infty} L_{ij}^{\eta\eta}(h^{\eta\eta}) \eta_i \eta_j = 0 \quad (\text{D1})$$

The operators in above equation are defined as

$$L_{ij}^{\xi\xi}(h^{\xi\xi}) = e^{-Y^{(0)}} C^{(0)} q^{(0)} \frac{\partial h_{ij}^{\xi\xi}}{\partial t} + e^{-Y^{(0)}} C_i^{(0)} q_i^{\xi} \frac{\partial h_j^{\xi}}{\partial t} + e^{-Y^{(0)}} C^{(0)} \frac{\partial h^{(0)}}{\partial t} q_{ij}^{\xi\xi} + e^{-Y^{(0)}} q^{(0)} C_i^{\xi} \frac{\partial h_j^{\xi}}{\partial t} + e^{-Y^{(0)}} \frac{\partial h^{(0)}}{\partial t} C_i^{\xi} q_j^{\xi} + e^{-Y^{(0)}} q^{(0)} \frac{\partial h^{(0)}}{\partial t} C_{ij}^{\xi\xi} - \nabla^2 h_{ij}^{\xi\xi} - \nabla Y^{(0)} \cdot \nabla h_{ij}^{\xi\xi} - \nabla Y_i^{\xi} \cdot \nabla h_j^{\xi} - \nabla Y_{ij}^{\xi\xi} \cdot \nabla (h^{(0)} + z) - g e^{-Y^{(0)}} q_{ij}^{\xi\xi} \quad (\text{D2})$$

$$L_{ij}^{\eta\eta}(h^{\eta\eta}) = e^{-Y^{(0)}} C^{(0)} q^{(0)} \frac{\partial h_{ij}^{\eta\eta}}{\partial t} + e^{-Y^{(0)}} C_i^{\eta} q_i^{\eta} \frac{\partial h_j^{\eta}}{\partial t} + e^{-Y^{(0)}} C^{(0)} q_{ij}^{\eta\eta} \frac{\partial h^{(0)}}{\partial t} + e^{-Y^{(0)}} q^{(0)} C_i^{\eta} \frac{\partial h_j^{\eta}}{\partial t} + e^{-Y^{(0)}} C_i^{\eta} q_j^{\eta} \frac{\partial h^{(0)}}{\partial t} + e^{-Y^{(0)}} q^{(0)} C_{ij}^{\eta\eta} \frac{\partial h^{(0)}}{\partial t} - \nabla^2 h_{ij}^{\eta\eta} - \nabla Y^{(0)} \cdot \nabla h_{ij}^{\eta\eta} - \nabla Y_i^{\eta} \cdot \nabla h_j^{\eta} - \nabla Y_{ij}^{\eta\eta} \cdot \nabla (h^{(0)} + z) - g e^{-Y^{(0)}} q_{ij}^{\eta\eta} \quad (\text{D3})$$

$$L_{ij}^{\xi\eta}(h^{\xi\eta}) = e^{-Y^{(0)}} C^{(0)} q^{(0)} \frac{\partial h_{ij}^{\xi\eta}}{\partial t} + e^{-Y^{(0)}} C^{(0)} \left( q_i^{\xi} \frac{\partial h_j^{\eta}}{\partial t} + q_j^{\eta} \frac{\partial h_i^{\xi}}{\partial t} \right) + e^{-Y^{(0)}} C^{(0)} q_{ij}^{\xi\eta} \frac{\partial h^{(0)}}{\partial t} + e^{-Y^{(0)}} q^{(0)} \left( \frac{\partial h_i^{\xi}}{\partial t} C_j^{\eta} + C_i^{\xi} \frac{\partial h_j^{\eta}}{\partial t} \right) + e^{-Y^{(0)}} (C_i^{\xi} q_j^{\eta} + C_j^{\eta} q_i^{\xi}) \frac{\partial h^{(0)}}{\partial t} + e^{-Y^{(0)}} q^{(0)} \frac{\partial h^{(0)}}{\partial t} C_{ij}^{\xi\eta} - \nabla^2 h_{ij}^{\xi\eta} - \nabla Y^{(0)} \cdot \nabla h_{ij}^{\xi\eta} - (\nabla Y_i^{\xi} \cdot \nabla h_j^{\eta} + \nabla Y_j^{\eta} \cdot \nabla h_i^{\xi}) - \nabla Y_{ij}^{\xi\eta} \cdot \nabla (h^{(0)} + z) - g e^{-Y^{(0)}} q_{ij}^{\xi\eta} \quad (\text{D4})$$

### Appendix E

The expectation of the normal random variables can be written as

$$\langle \xi_i \eta_j \xi_m \xi_n \rangle = \langle \eta_j \rangle \langle \xi_i \xi_m \xi_n \rangle = 0, \quad (\text{E1})$$

$$\langle \eta_i \eta_j \xi_m \xi_n \rangle = \langle \eta_i \eta_j \rangle \langle \xi_m \xi_n \rangle = \delta_{ij} \delta_{mn}$$

$$\langle \xi_i \xi_j \xi_m \xi_n \rangle = \delta_{ij} \delta_{mn} + \delta_{im} \delta_{jn} + \delta_{in} \delta_{jm}$$

By multiplying  $\xi_m \xi_n (m, n, = 1, 2, 3, \dots)$  of the both side of Eq. (41) and taking expectation, we have

$$\sum_{i,j=1}^{\infty} L_{ij}^{\xi\xi}(h^{\xi\xi})(\delta_{ij}\delta_{mn} + \delta_{im}\delta_{jn} + \delta_{in}\delta_{jm}) + \sum_{i,j=1}^{\infty} L_{ij}^{\eta\eta}(h^{\eta\eta})\delta_{ij}\delta_{mn} = 0, \quad m, n = 1, 2, \dots$$

By using the properties (E1) of the Kronecker delta function, we obtain

$$L_{mm}^{\xi\xi}(h^{\xi\xi})\delta_{mn} + L_{mm}^{\xi\xi}(h^{\xi\xi}) + L_{mm}^{\xi\xi}(h^{\xi\xi}) + L_{mm}^{\eta\eta}(h^{\eta\eta})\delta_{mn} = 0, \quad m, n = 1, 2, \dots \quad (E2)$$

Similarly, by multiplying the second order equation by  $\eta_m \eta_n$  and rearranging, we have

$$L_{mm}^{\eta\eta}(h^{\eta\eta})\delta_{mn} + L_{mm}^{\eta\eta}(h^{\eta\eta}) + L_{mm}^{\eta\eta}(h^{\eta\eta}) + L_{mm}^{\xi\xi}(h^{\xi\xi})\delta_{mn} = 0, \quad m, n = 1, 2, \dots \quad (E3)$$

Because of the symmetry of  $L_{mn}^{\xi\xi}$  and  $L_{mn}^{\eta\eta}$  about  $m$  and  $n$ , (E2) and (E3) can be written as

$$L_{mn}^{\xi\xi}(h^{\xi\xi}) + L_{mn}^{\eta\eta}(h^{\eta\eta}) = 0, \quad m \geq n \geq 1 \quad (E4)$$

The equation for  $h_{ij}$  and the corresponding boundary and initial conditions can be written as Eq. (43) with  $Q_{ij}$  and  $g_{ij}$  are defined by

$$g_{ij} = -e^{-Y^{(0)}} \left[ \bar{\alpha} g + (q^{(0)} C_{21} - \bar{\alpha} C^{(0)}) \frac{\partial h^{(0)}}{\partial t} \right] h_{ij} + \bar{\alpha} \nabla(h^{(0)} + z) \cdot \nabla h_{ij} + e^{-Y^{(0)}} \left( g - C^{(0)} \frac{\partial h^{(0)}}{\partial t} \right) z_{ij}^{(1)} - e^{-Y^{(0)}} q^{(0)} \frac{\partial h^{(0)}}{\partial t} z_{ij}^{(2)} + \nabla(h^{(0)} + z) \cdot \nabla z_{ij}^{(3)} + \frac{1}{2} (z_{ij}^{(4)} + z_{ji}^{(4)}), \quad i \geq j \geq 1 \quad (E5)$$

$$z_{ij}^{(1)} = \frac{1}{2} Y_i^\xi Y_j^\xi - \frac{1}{2} (\alpha_i h_j^\eta + \alpha_j h_i^\eta) + \frac{1}{2} Y_i^\eta Y_j^\eta \quad (E6)$$

$$z_{ij}^{(2)} = C_{22} h_i^\xi h_j^\xi + \frac{1}{2} C_{23} (h_i^\eta \alpha_j + h_j^\eta \alpha_i) + C_{24} \alpha_i \alpha_j$$

$$z_{ij}^{(3)} = \frac{1}{2} (\alpha_i h_j^\eta + \alpha_j h_i^\eta)$$

$$z_{ij}^{(4)} = \nabla Y_i^\eta \cdot \nabla h_j^\eta + \nabla Y_i^\xi \cdot \nabla h_j^\xi - e^{-Y^{(0)}} (C^{(0)} q_i^\xi + C_i^\xi q^{(0)}) \frac{\partial h_j^\xi}{\partial t} - e^{-Y^{(0)}} (C^{(0)} q_i^\eta + C_i^\eta q^{(0)}) \frac{\partial h_j^\eta}{\partial t} - e^{-Y^{(0)}} (C_i^\xi q_j^\xi + C_i^\eta q_j^\eta) \frac{\partial h^{(0)}}{\partial t}$$

and

$$Q_{ij} = - \left[ \frac{1}{2} (p_i^\xi \nabla h_j^\xi + p_i^\eta \nabla h_j^\eta + p_j^\xi \nabla h_i^\xi + p_j^\eta \nabla h_i^\eta) + z_{ij}^{(5)} \nabla(h^{(0)} + z) \right] \cdot \mathbf{n}|_{\Gamma_2} / p^{(0)} - h_{ij} [\bar{\alpha} \nabla(h^{(0)} + z)] \cdot \mathbf{n}|_{\Gamma_2} / p^{(0)} \quad (E7)$$

$$z_{ij}^{(5)} = \frac{1}{2} Y_i^{(\xi)} Y_j^{(\xi)} + \frac{1}{2} (\alpha_i h_j^\eta + \alpha_j h_i^\eta) + \frac{1}{2} Y_i^{(\eta)} Y_j^{(\eta)}$$

## References

- Bresler, E., Dagan, G., 1981. Convective and pore scale dispersive solute transport in unsaturated heterogeneous fields. *Water Resour. Res.* 17(6), 1683–1693.
- Brooks, R.H., Corey, A.T., 1964. Hydraulic properties of porous media, Hydrology paper 3, Colo. State University, Fort Collins.
- Cameron, R.H., Martin, W.T., 1947. The orthogonal development of nonlinear functionals in series of Fourier–Hermite functionals. *Ann. Math.* 48, 385–392.
- Dagan, G., 1984. Solute transport in heterogeneous porous formations. *J. Fluid Mech.* 145, 151–177.
- Dagan, G., 1989. *Flow and Transport in Porous Formations*, Springer, New York.
- Dagan, G., Bresler, E., 1979. Solute dispersion in unsaturated heterogeneous soil at field scale I. *Theory Soil Sci. Soc. Am. J.* 43, 461–467.
- Deodatis, G., 1989. Stochastic FEM sensitivity analysis of nonlinear dynamic problems. *ASCE J. Eng. Mech.* 4(3), 135–141.
- Gardner, W.R., 1958. Some steady state solutions of unsaturated moisture flow equations with application to evaporation from a water table. *Soil Sci.* 85, 228–232.
- Gelhar, L.W., Axness, C.L., 1983. Three-dimensional stochastic analysis of macrodispersion in aquifers. *Water Resour. Res.* 19(1), 161–180.
- van Genuchten, M.T., 1980. A closed-form equation for predicting the hydraulic conductivity of unsaturated soils. *Soil Sci. Soc. Am. J.* 44, 892–898.
- Ghanem, R.G., 1998. Probabilistic characterization of transport in heterogeneous media. *Comp. Meth. Appl. Mech. Eng.* 158, 199–220.
- Ghanem, R.G., 1999a. Ingredients for a general purpose stochastic finite elements implementation. *Comp. Meth. Appl. Mech. Eng.* 168, 19–34.

- Ghanem, R.G., 1999b. The nonlinear gaussian spectrum of log-normal stochastic processes and variables. *J. Appl. Mech., ASME* 66, 964–973.
- Ghanem, R.G., 1999c. Stochastic finite elements with multiple random non-Gaussian properties. *J. Eng. Mech. ASCE* 125(1), 26–40.
- Ghanem, R.G., Kruger, R., 1996. Numerical solution of spectral stochastic finite element systems. *Comp. Meth. Appl. Mech. Eng.* 129(3), 289–303.
- Ghanem, R.G., Dham, S., 1998. Stochastic finite element analysis for multiphase flow in heterogeneous media. *Transp Porous Media* 32, 239–262.
- Ghanem, R.G., Spanos, P.D., 1991a. Spectral stochastic finite-element formulation for reliability analysis. *J. Eng. Mech.* 117(10), 2351–2372.
- Ghanem, R.G., Spanos, P.D., 1991b. *Stochastic finite elements—a spectral approach*, Springer, Berlin.
- Jury, W.A., 1982. Simulation of solute transport using a transfer function model. *Water Resour. Res.* 18, 363–368.
- Li, B., Yeh, T.-C.J., 1998. Sensitivity and moment analyses of head in variably saturated regimes. *Adv. Water Resour.* 21, 477–485.
- Liedl, R., 1994. A conceptual perturbation model of water movement in stochastically heterogeneous soils. *Adv. Water Resour.* 17, 171–179.
- Loeve, M., 1977. *Probability Theory*, fourth ed., Springer, New York.
- Lu, Z., Zhang, D., 2002. Stochastic analysis of transient flow in heterogeneous, variably saturated porous media: the van Genuchten–Mualem constitutive model. *Vadose Zone J.* 1, 137–149.
- Mantoglou, A., 1992. A theoretical approach for modeling unsaturated flow in spatially variable soils: effective flow models in finite domains and nonstationarity. *Water Resour. Res.* 28(1), 251–267.
- Mantoglou, A., Gelhar, L.W., 1987. Stochastic modeling of large-scale transient unsaturated flow systems. *Water Resour. Res.* 23, 37–46.
- Mathies, H.G., Brenner, C.E., Bucher, C.G., Soares, C.G., 1997. Uncertainties in probabilistic numerical analysis of structures and solids-stochastic finite elements. *Struct. Safety* 19(3), 283–336.
- Neuman, S.P., Winter, C.L., Newman, C.M., 1987. Stochastic theory of field-scale Fickian dispersion in anisotropic porous media. *Water Resour. Res.* 23, 453–466.
- Roy, R.V., Grilli, S.T., 1997. Probabilistic analysis of flow in random porous media by stochastic boundary element. *Eng. Anal. Boundary Elem.* 19, 239–255.
- Russo, D., 1988. Determining soil hydraulic properties by parameter estimation: On the selection of a model for the hydraulic properties. *Water Resour. Res.* 24(3), 453–459.
- Russo, D., 1993. Stochastic modeling of macrodispersion for solute transport in a heterogeneous unsaturated porous formation. *Water Resour. Res.* 29, 383–397.
- Russo, D., 1995. On the velocity covariance and transport modeling in heterogeneous anisotropic porous formations, 2, unsaturated flow. *Water Resour. Res.* 31(1), 139–145.
- Wiener, N., 1938. The homogeneous chaos. *Am. J. Math.* 60, 897–936.
- Winter, C.L., Newman, C.M., Neuman, S.P., 1984. A perturbation expansion for diffusion in a random velocity field. *SIAM J. Appl. Math.* 44(2), 411–424.
- Yang, J., Zhang, R., Wu, J., 1996. A analytical solution of macrodispersivity for adsorbing solute transport in unsaturated soils. *Water Resour. Res.* 32, 355–362.
- Yang, J., Zhang, R., Wu, J., 1997. Stochastic analysis of adsorbing solute transport in three-dimensional heterogeneous unsaturated soils. *Water Resour. Res.* 33, 1947–1956.
- Yeh, T.-C., Gelhar, L.W., Gutjahr, A.L., 1985a. Stochastic analysis of unsaturated flow in heterogeneous soils, 1, statistically isotropic media. *Water Resour. Res.* 21(4), 447–456.
- Yeh, T.-C., Gelhar, L.W., Gutjahr, A.L., 1985b. Stochastic analysis of unsaturated flow in heterogeneous soils, 2, statistically anisotropic media with variable  $a$ . *Water Resour. Res.* 21(4), 457–464.
- Yeh, T.-C., Gelhar, L.W., Gutjahr, A.L., 1985c. Stochastic analysis of unsaturated flow in heterogeneous soils, 3, observation and Application. *Water Resour. Res.* 21(4), 465–471.
- Zhang, D., 1998. Numerical solutions to statistical moment equations of groundwater flow in nonstationary, bounded heterogeneous media. *Water Resour. Res.* 34(3), 529–538.
- Zhang, D., 1999. Nonstationary stochastic analysis of transient unsaturated flow in randomly heterogeneous media. *Water Resour. Res.* 35(4), 1127–1141.
- Zhang, D., 2002. *Stochastic Methods for Flow in Porous Media: Coping With Uncertainties*, Academic, San Diego, CA, 350 pp.
- Zhang, D., Lu, Z., 2002. Stochastic analysis of flow in a heterogeneous unsaturated–saturated system. *Water Resour. Res.* 38(2), 101029.
- Zhang, D., Lu, Z., 2004. An efficient, higher-order perturbation approach for flow in randomly heterogeneous porous media via Karhunen-Loeve decomposition. *J. Comput. Phys.* 194(2), 773–794.
- Zhang, D., Winter, C.L., 1998. Nonstationary stochastic analysis of steady state flow through variably saturated, heterogeneous media. *Water Resour. Res.* 34, 1091–1100.
- Zhang, D., Wallstrom, T.C., Winter, C.L., 1998. Stochastic analysis of steady state unsaturated flow in heterogeneous media: comparison of the Brooks–Corey and Gardner–Russo models. *Water Resour. Res.* 34(6), 1437–1449.